On the energy-minimizing strains in martensitic microstructures-Part 2: Geometrically linear theory

Michaël Peigney

▶ **To cite this version:**

Michaël Peigney. On the energy-minimizing strains in martensitic microstructures-Part 2: Geometrically linear theory. Journal of the Mechanics and Physics of Solids, 2013, 61 (6), pp.1511-1530. 10.1016/j.jmps.2012.12.011 . hal-00813545

HAL Id: hal-00813545

https://enpc.hal.science/hal-00813545

Submitted on 18 Sep 2015

HAL is a multi-disciplinary open access archive for the deposit and dissemination of scientific research documents, whether they are published or not. The documents may come from teaching and research institutions in France or abroad, or from public or private research centers.

L'archive ouverte pluridisciplinaire **HAL**, est destinée au dépôt et à la diffusion de documents scientifiques de niveau recherche, publiés ou non, émanant des établissements d'enseignement et de recherche français ou étrangers, des laboratoires publics ou privés.

On the energy-minimizing strains in martensitic microstructures - Part 2: Geometrically linear theory

Michaël Peigney

Université Paris-Est, Laboratoire Navier (Ecole des Ponts ParisTech, IFSTTAR, CNRS), F-77455 Marne-la-Vallée Cedex 2, France

Abstract

This paper addresses the theoretical prediction of the set of energy-minimizing (or stress-free) strains that can be realized by martensitic microstructure. Polyconvexification and related notions are used to derive some upper bounds (in the sense of inclusion of sets). Lower bounds are obtained from lamination techniques. The geometrically linear setting (infinitesimal strains) is considered in the present Part 2. Three-, four-, and twelve-well problems are considered. In particular, the structure of the set of energy-minimizing strains in cubic to monoclinic transformations is investigated in detail. That investigation is notably supported by three-dimensional vizualisations obtained by considering four-well restrictions.

Keywords: Energy minimization, Lamination, Microstructures, Phase transformation, Shape-memory alloys

1. Introduction

The peculiar properties of shape memory alloys are the macroscopic result of a diffusion-less solid/solid phase transformation that occurs at a microscopic level. Adopting the framework of non-linear elasticity, the microscopic behavior is classically described by a multi-well free energy Ψ. The macroscopic (or effective) free energy is then obtained as the relaxation (or quasiconvexification) of Ψ. Because of the non-convex structure of Ψ, the relaxation procedure is notoriously difficult to perform. Exact solutions are only known in few special cases. This paper focuses on the set of strains that minimize the macroscopic energy. Those so-called recoverable strains can be interpreted as stress-free macroscopic strains. As explained by Bhattacharya

and Kohn (1997), they play an important role in the properties of shape memory alloys.

The problem can be formulated either in the geometrically non-linear setting (finite strains) or in the geometrically linear setting (infinitesimal strains). The present Part 2 is devoted to the geometrically linear theory, whereas the geometrically non-linear theory has been considered in Part 1 (Peigney, 2013). Although the geometrically non-linear theory is more accurate, the problem is significantly more tractable in the geometrically linear theory. Consider for instance the case of n geometrically compatible phases. In the geometrically linear setting, it can be proved that the set of energy-minimizing macroscopic strains is equal to the convex hull of the strains that minimize Ψ (Bhattacharya, 1993). In contrast, in the geometrically non-linear setting, the problem is much more complex and has been solved exactly only in the case $n = 2$ (Ball and James, 1992). It has to be mentioned that, even in the geometrically linear setting, substantial difficulties remain where the phases are not all pairwise compatible: analytical expressions have been only obtained in the cases of two and three phases (Kohn, 1991; Smyshlyaev and Willis, 1998).

The outline of the present Part 2 is as follows. Using distinctive properties of the relaxation, we first derive a general upper bound (denoted by $P\mathcal{K}$) on the set of strains that minimize the macroscopic energy (Section 2). This is accomplished by adapting a method used in Part 1 to the geometrically linear theory. That upper bound is compared with existing bounds from the literature. In particular, for the three-well problem (Section 3), the bound obtained is shown to coincide with the results of Smyshlyaev and Willis (1998). Four-well problems are considered in Section 4. The upper bound $P\mathcal{K}$ is compared with lower bounds constructed by a sequential lamination algorithm. Three-dimensional visualizations of the various bounding sets are given for some examples related to the cubic to monoclinic transformations. Those examples serve two purposes. First, they illustrate the gap between the lower and upper bounds considered, giving an appreciation of those bounds. Second, they provide a first insight in the full study of the twelve-well problems corresponding to cubic to monoclinic transformations, which is the focus of Section 5. Taking the 12 variants into account adds some complications in the derivation of meaningful bounds. In particular, the sequential lamination algorithm introduced in Section 4 cannot be used directly as it involves prohibitive calculation costs. An alternative strategy is detailed for constructing relevant lower bounds in that case. The structure

of the bounds obtained is investigated in detail, distinguishing the cases of monoclinic-I and monoclinic-II martensite.

2. Upper bound on $Q\mathcal{K}$ in the geometrically linear theory

Let Ψ denote the free energy density of the material at the microscopic level. To account for the phase transformation between austenite and martensite, Ψ is generally modeled as a function with multiple wells. We denote by $\mathcal{K}$ the set of strains that minimize Ψ. In the geometrically linear setting, $\mathcal{K}$ is a discrete set, i.e.

$$\mathcal{K} = \{\boldsymbol{e}_1, \cdots, \boldsymbol{e}_n\}. \tag{2.1}$$

At a temperature below the transformation temperature, the strains $\boldsymbol{e}_1, \cdots, \boldsymbol{e}_n$ in (2.1) are the transformation strains of the martensitic variants.

Consider a crystal occupying a domain Ω. The effective free energy of the material is the relaxation (or quasiconvexification) of Ψ, defined as

$$Q\Psi(\bar{\boldsymbol{e}}) = \inf_{\boldsymbol{e}\in\mathcal{A}(\bar{\boldsymbol{e}})} \frac{1}{|\Omega|}\int_\Omega \Psi(\boldsymbol{e})\, d\boldsymbol{x} \tag{2.2}$$

where

$$\begin{aligned}\mathcal{A}(\bar{\boldsymbol{e}}) = \{\boldsymbol{e}| \quad & \exists \boldsymbol{u}(\boldsymbol{x}) \in W^{1,\infty}(\Omega, \mathbb{R}^3) \text{ such that} \\ & \boldsymbol{e} = (\nabla\boldsymbol{u} + \nabla^T\boldsymbol{u})/2 \text{ in } \Omega; \boldsymbol{u}(\boldsymbol{x}) = \bar{\boldsymbol{e}}.\boldsymbol{x} \text{ on } \partial\Omega\}.\end{aligned} \tag{2.3}$$

The multiple-well structure of Ψ entails that the infimum in (2.2) is generally not attained, which makes the calculation of $Q\Psi$ a far from trivial matter. Also note that $Q\Psi$ is independent on the domain Ω considered (see e.g. Dacorogna (2008) and references therein).

In this paper we are interested in estimating the set of effective strains that minimize $Q\Psi$. That set, denoted by $Q\mathcal{K}$, is referred to as the quasiconvex hull of $\mathcal{K}$. The first step in our study is to derive a general upper bound on $Q\mathcal{K}$. This is accomplished by using a distinctive property of $Q\mathcal{K}$, namely that any strain $\bar{\boldsymbol{e}}$ in $Q\mathcal{K}$ can be written as

$$\bar{\boldsymbol{e}} = \int_{\mathbb{R}^{3\times3}_s} \boldsymbol{e} d\nu(\boldsymbol{e}) \tag{2.4}$$

for some Young measure ν supported on $\mathcal{K}$ (Ball and James, 1992; Müller, 1999). A notable consequence of that property is that $Q\mathcal{K}$ only depends on Ψ

through its set $\mathcal{K}$ of minimizers. Young measures notably have the following properties (Kinderlehrer and Pedregal, 1991):

$$\nu \geq 0; \int_{\mathbb{R}^{3\times 3}_s} d\nu(\boldsymbol{e}) = 1; \tag{2.5}$$

$$h(\int_{\mathbb{R}^{3\times 3}_s} \boldsymbol{e} d\nu(\boldsymbol{e})) \leq \int_{\mathbb{R}^{3\times 3}_s} h(\boldsymbol{e}) d\nu(\boldsymbol{e}) \text{ for any quasiconvex function } h. \tag{2.6}$$

In the present case, $\mathcal{K}$ has the discrete structure (2.1). The measure ν in (2.4) is supported on $\mathcal{K}$ and therefore can be written as

$$\nu = \sum_{r=1}^{n} \theta_r \delta_{\boldsymbol{e}_r} \tag{2.7}$$

where $\delta_{\boldsymbol{e}_r}$ is the Dirac mass at $\boldsymbol{e}_r$. The property (2.5) implies that $\boldsymbol{\theta} = (\theta_1, \cdots, \theta_n)$ belongs to the set $\mathcal{T}_n$ defined as

$$\mathcal{T}_n = \{\boldsymbol{\theta} = (\theta_1, \cdots, \theta_n) | \theta_r \geq 0; \sum_{r=1}^{n} \theta_r = 1\}.$$

Substituting (2.7) in (2.4)-(2.6) shows that any strain $\bar{\boldsymbol{e}}$ in $Q\mathcal{K}$ can be written as

$$\bar{\boldsymbol{e}} = \sum_{r=1}^{n} \theta_r \boldsymbol{e}_r$$

for some $\boldsymbol{\theta} \in \mathcal{T}_n$ verifying

$$h(\bar{\boldsymbol{e}}) \leq \sum_{r=1}^{n} \theta_r h(\boldsymbol{e}_r) \text{ for any quasiconvex function } h. \tag{2.8}$$

Recall that a function h is quasiconvex in the linearized strain $\boldsymbol{e}$ if

$$|\Omega| h(\bar{\boldsymbol{e}}) \leq \int_{\Omega} h(\boldsymbol{e})\, d\boldsymbol{x} \text{ for all } \bar{\boldsymbol{e}} \text{ and } \boldsymbol{e} \in \mathcal{A}(\bar{\boldsymbol{e}}). \tag{2.9}$$

Let $\boldsymbol{e}^*$ denote the adjugate of $\boldsymbol{e}$, defined by the relations

$$e^*_{ii} = e_{jj}e_{kk} - e^2_{jk},\ e^*_{jk} = e_{ji}e_{ki} - e_{jk}e_{ii},$$

for any $\{i, j, k\}$ permutation of $\{1, 2, 3\}$. We use the notation $\boldsymbol{M} \geq 0$ to indicate that a second-order symmetric tensor $\boldsymbol{M}$ is positive, i.e. satisfies

$\boldsymbol{u}.\boldsymbol{M}.\boldsymbol{u} \geq 0$ for all vectors $\boldsymbol{u}$. It can be verified that the function $\boldsymbol{e} \mapsto -\boldsymbol{a} : \boldsymbol{e}^*$ is quasiconvex provided that $\boldsymbol{a} \geq 0$ (see e.g. Peigney (2008)). Using such functions in (2.8) gives

$$0 \leq \boldsymbol{a} : (\bar{\boldsymbol{e}}^* - \sum_{r=1}^{n} \theta_r \boldsymbol{e}_r^*) \text{ for any } \boldsymbol{a} \geq 0,$$

and therefore that

$$\bar{\boldsymbol{e}}^* - \sum_{r=1}^{n} \theta_r \boldsymbol{e}_r^* \geq 0.$$

That relation can be rewritten in a more convenient form. Using the equality $\sum_r \theta_r = 1$ and the fact that the function $\boldsymbol{e} \mapsto \boldsymbol{e}^*$ is quadratic, we have

$$\bar{\boldsymbol{e}}^* - \sum_{r} \theta_r \boldsymbol{e}_r^* = (\sum_{r} \theta_r \boldsymbol{e}_r)^* - \sum_{r} \theta_r \boldsymbol{e}_r^* = -\frac{1}{2} \sum_{r,s} \theta_r \theta_s (\boldsymbol{e}_r - \boldsymbol{e}_s)^*.$$

The conclusion is that any $\bar{\boldsymbol{e}}$ in $Q\mathcal{K}$ can be written as $\bar{\boldsymbol{e}} = \sum_{r=1}^{n} \theta_r \boldsymbol{e}_r$ for some $\boldsymbol{\theta} \in \mathcal{T}_n$ verifying $-\sum_{r,s} \theta_r \theta_s (\boldsymbol{e}_r - \boldsymbol{e}_s)^* \geq 0$. The set $Q\mathcal{K}$ is thus included in the set $P\mathcal{K}$ defined as

$$P\mathcal{K} = \{\sum_{r=1}^{n} \theta_r \boldsymbol{e}_r | \boldsymbol{\theta} \in \mathcal{T}_n; -\sum_{r,s=1}^{n} \theta_r \theta_s (\boldsymbol{e}_r - \boldsymbol{e}_s)^* \geq 0\}. \tag{2.10}$$

The notation $P\mathcal{K}$ is motivated by the fact that the set in (2.10) is related to the notion of polyconvexity used in the geometrically non-linear theory (see Part 1). From (2.10) it can be seen that $P\mathcal{K}$ is included in the convex hull $C\mathcal{K}$ of $\{\boldsymbol{e}_1, \cdots, \boldsymbol{e}_n\}$, given by $C\mathcal{K} = \{\sum_{r=1}^{n} \theta_r \boldsymbol{e}_r | \boldsymbol{\theta} \in \mathcal{T}_n\}$. Moreover, $P\mathcal{K}$ is equal to $C\mathcal{K}$ if $-(\boldsymbol{e}_r - \boldsymbol{e}_s)^*$ is positive for all $\{r, s\}$. Let us interpret this last condition: for a fixed pair $\{r, s\}$, the symmetric tensor $\boldsymbol{e}_r - \boldsymbol{e}_s$ can be decomposed as $\boldsymbol{e}_r - \boldsymbol{e}_s = \sum_{i=1}^{3} \epsilon_i \boldsymbol{u}_i \otimes \boldsymbol{u}_i$ where $(\epsilon_1, \epsilon_2, \epsilon_3)$ are the eigenvalues of $\boldsymbol{e}_r - \boldsymbol{e}_s$ and $(\boldsymbol{u}_1, \boldsymbol{u}_2, \boldsymbol{u}_3)$ is an orthonormal basis. The adjugate tensor $(\boldsymbol{e}_r - \boldsymbol{e}_s)^*$ is then equal to $\epsilon_2 \epsilon_3 \boldsymbol{u}_1 \otimes \boldsymbol{u}_1 + \epsilon_1 \epsilon_3 \boldsymbol{u}_2 \otimes \boldsymbol{u}_2 + \epsilon_1 \epsilon_2 \boldsymbol{u}_3 \otimes \boldsymbol{u}_3$. Consequently, $-(\boldsymbol{e}_r - \boldsymbol{e}_s)^*$ is positive if and only if $\epsilon_i \epsilon_j \leq 0$ for all $i \neq j$, i.e. if and only if one eigenvalue is equal to 0 and the two others are of opposite sign. This last condition can be shown (Bhattacharya, 1993) to be equivalent to the fact that the strains $\boldsymbol{e}_r$ and $\boldsymbol{e}_s$ are *compatible*, i.e. there exists some vectors $(\boldsymbol{u}, \boldsymbol{v})$ such that

$$\boldsymbol{e}_r - \boldsymbol{e}_s = \boldsymbol{u} \otimes \boldsymbol{v} + \boldsymbol{v} \otimes \boldsymbol{u}. \tag{2.11}$$

Hence $P\mathcal{K}$ is equal to $C\mathcal{K}$ if the strains $\{\boldsymbol{e}_1, \cdots, \boldsymbol{e}_n\}$ are pairwise compatible. In that case, it is actually known that $Q\mathcal{K} = C\mathcal{K}$ (Bhattacharya, 1993).

2.1. Relations with existing bounds on the energy

Any *lower* bound $Q^-\Psi$ on the relaxation $Q\Psi$ automatically generates an *upper* bound on $Q\mathcal{K}$ (in the sense of inclusion of sets). Indeed, if $Q^-\Psi$ is such that $Q^-\Psi \leq Q\Psi$, then $Q\mathcal{K} \subset \{\bar{\boldsymbol{e}} | Q^-\Psi(\bar{\boldsymbol{e}}) \leq 0\}$. It is interesting to compare such an upper bound with the bound $P\mathcal{K}$ in (2.10). In the geometrically linear setting, lower bounds on $Q\Psi$ have been proposed in the case where

$$\Psi(\boldsymbol{e}) = \min_{1 \leq r \leq n+1} \Psi_r \tag{2.12}$$

with

$$\begin{aligned} \Psi_r(\boldsymbol{e}) &= \frac{1}{2}(\boldsymbol{e} - \boldsymbol{e}_r) : \boldsymbol{L} : (\boldsymbol{e} - \boldsymbol{e}_r) \text{ for } r \leq n, \\ \Psi_{n+1}(\boldsymbol{e}) &= \frac{1}{2}\boldsymbol{e} : \boldsymbol{L} : \boldsymbol{e} + m. \end{aligned} \tag{2.13}$$

In those expressions, Ψ_r and Ψ_{n+1} are the free energy of martensite variant r and of the austenite, respectively. At a temperature below the transformation temperature, the minimum energy m of the austenite is strictly positive. The tensor $\boldsymbol{L}$ is a symmetric positive definite elasticity tensor, assumed to take the same value for all the phases. In that case, as detailed by Govindjee et al. (2003), the relaxation $Q\Psi$ has the structure

$$Q\Psi(\bar{\boldsymbol{e}}) = \inf_{\boldsymbol{\theta} \in \mathcal{T}_{n+1}} \sum_{r=1}^{n+1} \theta_r \Psi_r(\bar{\boldsymbol{e}}) + h(\boldsymbol{\theta}) \tag{2.14}$$

where $h(\boldsymbol{\theta})$ can be interpreted as a mixing energy between the phases. Solving the relaxation problem is equivalent to determining the function h. Govindjee et al. (2003) considered the lower bound h_0 on h provided by the following formula:

$$h_0(\boldsymbol{\theta}) = \frac{1}{2} \sum_{r,s=1}^{n} \theta_r \theta_s \boldsymbol{e}_r : \boldsymbol{L} : \boldsymbol{e}_s - \frac{1}{2} \sum_{r=1}^{n} \theta_r \boldsymbol{e}_r : \boldsymbol{L} : \boldsymbol{e}_r. \tag{2.15}$$

The resulting lower bound on $Q\Psi$ is equal to the convexification of Ψ, as defined by

$$C\Psi(\bar{\boldsymbol{e}}) = \inf_{\boldsymbol{\theta} \in \mathcal{T}_{n+1}} C\Psi(\bar{\boldsymbol{e}}, \boldsymbol{\theta}) \tag{2.16}$$

with

$$C\Psi(\bar{\boldsymbol{e}}, \boldsymbol{\theta}) = \frac{1}{2}(\bar{\boldsymbol{e}} - \sum_{r=1}^{n} \theta_r \boldsymbol{e}_r) : \boldsymbol{L} : (\bar{\boldsymbol{e}} - \sum_{r=1}^{n} \theta_r \boldsymbol{e}_r) + m\theta_{n+1}.$$

The upper bound on $Q\mathcal{K}$ that is deduced from (2.16) is the convex hull $C\mathcal{K}$. If the strains $(\boldsymbol{e}_1, \cdots, \boldsymbol{e}_n)$ are not all pairwise compatible, the sets $Q\mathcal{K}$ and $P\mathcal{K}$ may be strictly smaller than $C\mathcal{K}$ (see Section 4 for some examples). A lower bound h_1 that improves on (2.15) has been proposed by Peigney (2009). The corresponding lower bound on $Q\Psi$ is expressed as

$$Q\Psi(\bar{\boldsymbol{e}}) \geq \inf_{\boldsymbol{\theta} \in \mathcal{T}_{n+1}} C\Psi(\bar{\boldsymbol{e}}, \boldsymbol{\theta}) + h_1(\boldsymbol{\theta})$$

where

$$h_1(\boldsymbol{\theta}) = \sup_{\boldsymbol{a} \geq 0 | \boldsymbol{L} - \boldsymbol{K}(\boldsymbol{a}) \geq 0} \frac{1}{2} \sum_{r=1}^{n} \theta_r \boldsymbol{e}_r : \boldsymbol{M}(\boldsymbol{a}) : \boldsymbol{e}_r - \frac{1}{2} \sum_{r,s=1}^{n} \theta_r \theta_s \boldsymbol{e}_r : \boldsymbol{M}(\boldsymbol{a}) : \boldsymbol{e}_s. \tag{2.17}$$

In that equation, $\boldsymbol{K}(\boldsymbol{a})$ is the symmetric fourth-order tensor such that $(1/2)\bar{\boldsymbol{e}} : \boldsymbol{K}(\boldsymbol{a}) : \bar{\boldsymbol{e}} = -\boldsymbol{a} : \bar{\boldsymbol{e}}^*$ for all $\bar{\boldsymbol{e}}$, and $\boldsymbol{M}(\boldsymbol{a})$ is defined by

$$\boldsymbol{M}(\boldsymbol{a}) = -\boldsymbol{K}(\boldsymbol{a}) - \boldsymbol{K}(\boldsymbol{a}) : (\boldsymbol{L} - \boldsymbol{K}(\boldsymbol{a}))^{-1} : \boldsymbol{K}(\boldsymbol{a}). \tag{2.18}$$

The corresponding bound on $Q\mathcal{K}$ is given by

$$\{\sum_{r=1}^{n} \theta_r \boldsymbol{e}_r | \boldsymbol{\theta} \in \mathcal{T}_{n+1}; \theta_{n+1} = 0; h_1(\boldsymbol{\theta}) \leq 0\}. \tag{2.19}$$

That bound is now compared with the bound $P\mathcal{K}$ in (2.10). Consider a given $\boldsymbol{\theta} \in \mathcal{T}_{n+1}$ such that $h_1(\boldsymbol{\theta}) \leq 0$ and $\theta_{n+1} = 0$. We have

$$0 \geq \sum_{r,s=1}^{n} \theta_r \theta_s (\boldsymbol{e}_r - \boldsymbol{e}_s) : \boldsymbol{M}(\boldsymbol{a}) : (\boldsymbol{e}_r - \boldsymbol{e}_s) \tag{2.20}$$

for any $\boldsymbol{a} \geq 0$ verifying $\boldsymbol{L} - \boldsymbol{K}(\boldsymbol{a}) \geq 0$. Let $\boldsymbol{a}^0 \geq 0$ be fixed. For t positive sufficiently small, the tensor $\boldsymbol{L} - \boldsymbol{K}(t\boldsymbol{a}^0)$ is positive. Moreover, at the first order in t, the tensor $\boldsymbol{M}(t\boldsymbol{a}^0)$ is equal to $-t\boldsymbol{K}(\boldsymbol{a}^0)$. We thus obtain from (2.20) that

$$0 \geq \sum_{r,s=1}^{n} -\theta_r \theta_s (\boldsymbol{e}_r - \boldsymbol{e}_s) : \boldsymbol{K}(\boldsymbol{a}^0) : (\boldsymbol{e}_r - \boldsymbol{e}_s),$$

i.e. that $0 \leq -\boldsymbol{a}^0 : (\sum_{r,s} \theta_r \theta_s (\boldsymbol{e}_r - \boldsymbol{e}_s)^*)$. This proves that the tensor $-\sum_{r,s=1}^{n} \theta_r \theta_s (\boldsymbol{e}_r - \boldsymbol{e}_s)^*$ is positive. Consequently, any strain in the set (2.19)

is in the $P\mathcal{K}$ defined by (2.10). Conversely, consider a given $\boldsymbol{\theta} \in \mathcal{T}_n$ such that $0 \leq -\sum_{r,s=1}^{n} \theta_r \theta_s (\boldsymbol{e}_r - \boldsymbol{e}_s)^*$. Setting $\theta_{n+1} = 0$, we have from the definition (2.18) of $\boldsymbol{M}(\boldsymbol{a})$:

$$\begin{aligned} 4h(\boldsymbol{\theta}) &= \sum_{r,s=1}^{n+1} \theta_r \theta_s (\boldsymbol{e}_r - \boldsymbol{e}_s) : \boldsymbol{M}(\boldsymbol{a}) : (\boldsymbol{e}_r - \boldsymbol{e}_s) \\ &= \boldsymbol{a} : (\sum_{r,s=1}^{n} \theta_r \theta_s (\boldsymbol{e}_r - \boldsymbol{e}_s)^*) - \sum_{r,s=1}^{n} \boldsymbol{\tau}_{rs} : (\boldsymbol{L} - \boldsymbol{K}(\boldsymbol{a}))^{-1} : \boldsymbol{\tau}_{rs} \end{aligned} \tag{2.21}$$

where $\boldsymbol{\tau}_{rs} = \boldsymbol{K}(\boldsymbol{a}) : (\boldsymbol{e}_r - \boldsymbol{e}_s)$. For any $\boldsymbol{a} \geq 0$ such that $\boldsymbol{L} - \boldsymbol{K}(\boldsymbol{a}) \geq 0$, the two terms on the right-hand side of (2.21) are negative. Therefore, any strain in $P\mathcal{K}$ is in the set (2.19). The conclusion is that the bound $P\mathcal{K}$ in (2.10) coincides with the set deduced from the energy bound (2.17). Note however that the latter only applies when the microscopic energy is piecewise quadratic of the form (2.12), whereas the bound $P\mathcal{K}$ does not rely on that assumption.

3. The tree-well problem

The quasiconvexification of the free energy Ψ in (2.12) has been thoroughly studied by Smyshlyaev and Willis (1998) in the case $n = 3$. Using a Hashin–Shtrickman type variational formulation and considering known restrictions on $\mathbb{H}$-measures, these authors derived a lower bound $Q_{SW}\Psi$ that improves on the convexification of Ψ, and obtained a sufficient condition for that lower bound $Q_{SW}\Psi$ to coincide with the exact value of $Q\Psi$. Here we consider an example given by Smyshlyaev and Willis (1998), for which the calculations can be done in closed form: the elasticity tensor $\boldsymbol{L}$ in (2.12) is taken as isotropic (i.e. $L_{ijpq} = \lambda \delta_{ij} \delta_{pq} + \mu(\delta_{ip}\delta_{jq} + \delta_{iq}\delta_{jp})$), and the strains $(\boldsymbol{e}_1, \boldsymbol{e}_2, \boldsymbol{e}_3)$ in (2.12) are taken as

$$\boldsymbol{e}_1 = \mathrm{diag}(\lambda_1, \lambda_2, \lambda_3) \ , \ \boldsymbol{e}_2 = \mathrm{diag}(\mu_1, \mu_2, \mu_3) \ , \boldsymbol{e}_3 = 0. \tag{3.1}$$

The eigenvalues λ_i and μ_i can always be represented in the form

$$\lambda_j = R_j \cos \frac{1}{2}\chi_j \ , \ \mu_j = -R_j \sin \frac{1}{2}\chi_j, \tag{3.2}$$

for some scalars R_j and χ_j. To alleviate the notations, we set:

$$s_i = \sin \frac{1}{2}\chi_i \ , \ c_i = \cos \frac{1}{2}\chi_i \ , \ s(i{+}j) = \sin \frac{1}{2}(\chi_i{+}\chi_j) \ , \ s(i{-}j) = \sin \frac{1}{2}(\chi_i{-}\chi_j). \tag{3.3}$$

We assume that the following condition, introduced by Smyshlyaev and Willis (1998), is satisfied for all permutation $\{i,j,k\}$ of $\{1,2,3\}$:

$$R_j R_k s(j-i)s(k-i) < 0. \tag{3.4}$$

The bound $Q_{SW}\Psi$ obtained by Smyshlyaev and Willis (1998) takes the following expression:

$$Q_{SW}\Psi(\bar{\boldsymbol{e}}) = \inf_{(\theta_1,\theta_2)\in\mathcal{T}_2'} \{\frac{1}{2}(\bar{\boldsymbol{e}} - \theta_1\boldsymbol{e}_1 - \theta_2\boldsymbol{e}_2) : \boldsymbol{L} : (\bar{\boldsymbol{e}} - \theta_1\boldsymbol{e}_1 - \theta_2\boldsymbol{e}_2) + \hat{I}(\theta_1,\theta_2)\} \tag{3.5}$$

with

$$\mathcal{T}_2' = \{(\theta_1,\theta_2) | 0 \le \theta_1; 0 \le \theta_2; \theta_1 + \theta_2 \le 1\}. \tag{3.6}$$

The function $\hat{I}$ in (3.5) is of the form

$$\hat{I}(\theta_1,\theta_2) = \inf_{(k_r,\phi_r)} \sum_{r=1}^{3} F(\phi_r) \tag{3.7}$$

where the infimum is taken over values (k_r,ϕ_r) such that $k_r \ge 0$ and

$$\begin{pmatrix} \theta_1(1-\theta_1) & -\theta_1\theta_2 \\ -\theta_1\theta_2 & \theta_2(1-\theta_2) \end{pmatrix} = \sum_{r=1}^{3} k_r \begin{pmatrix} \sin^2\frac{1}{2}\phi_r & \sin\frac{1}{2}\phi_r\cos\frac{1}{2}\phi_r \\ \sin\frac{1}{2}\phi_r\cos\frac{1}{2}\phi_r & \cos^2\frac{1}{2}\phi_r \end{pmatrix}. \tag{3.8}$$

The exact expression of the function F in (3.7) can be found in Smyshlyaev and Willis (1998)(eqn(7.16)). For our purpose, it is sufficient to mention that F is a positive function. Let $Q_{SW}\mathcal{K} = \{\bar{\boldsymbol{e}} | Q_{SW}\Psi(\bar{\boldsymbol{e}}) \le 0\}$ be the upper bound on $Q\mathcal{K}$ deduced from $Q_{SW}\Psi$. Since $\boldsymbol{L}$ and F are positive, $Q_{SW}\Psi(\bar{\boldsymbol{e}})$ is negative if and only if $\bar{\boldsymbol{e}} = \theta_1\boldsymbol{e}_1 + \theta_2\boldsymbol{e}_2$ for some $(\theta_1,\theta_2) \in \mathcal{T}_2'$ verifying $\hat{I}(\theta_1,\theta_2) = 0$. When the condition (3.4) is satisfied, it has been shown by Smyshlyaev and Willis (1998) that $\hat{I}(\theta_1,\theta_2) = 0$ if and only if the infimum over ϕ_r in (3.7) is attained for $\phi_r = \chi_r$. Consequently, the upper bound $Q_{SW}\mathcal{K}$ consists of tensors $\theta_1\boldsymbol{e}_1 + \theta_2\boldsymbol{e}_2$ for which $(\theta_1,\theta_2) \in \mathcal{T}_2'$ and there exists $k_r \ge 0$ verifying

$$\begin{pmatrix} \theta_1(1-\theta_1) & -\theta_1\theta_2 \\ -\theta_1\theta_2 & \theta_2(1-\theta_2) \end{pmatrix} = \sum_{r=1}^{3} k_r \begin{pmatrix} s_r^2 & s_r c_r \\ s_r c_r & c_r^2 \end{pmatrix}. \tag{3.9}$$

Let us now compare this result with the bound $P\mathcal{K}$ in (2.10). Define the tensor $\boldsymbol{E}(\theta_1,\theta_2)$ by

$$\boldsymbol{E}(\theta_1,\theta_2) = \theta_1(1-\theta_1-\theta_2)\boldsymbol{e}_1^* + \theta_2(1-\theta_1-\theta_2)\boldsymbol{e}_2^* + \theta_1\theta_2(\boldsymbol{e}_1 - \boldsymbol{e}_2)^*. \tag{3.10}$$

The set $P\mathcal{K}$ in (2.10) consists of tensors $\theta_1 \boldsymbol{e}_1 + \theta_2 \boldsymbol{e}_2$ such that $(\theta_1, \theta_2) \in \mathcal{T}_2'$ and $-\boldsymbol{E}(\theta_1, \theta_2) \geq 0$. Some simple calculations give

$$\begin{array}{rcl} \boldsymbol{e}_1^* & = & \mathrm{diag}(R_2R_3c_2c_3, R_1R_3c_1c_3, R_1R_2c_1c_2), \\ \boldsymbol{e}_2^* & = & \mathrm{diag}(R_2R_3s_2s_3, R_1R_3s_1s_3, R_1R_2s_1s_2), \\ (\boldsymbol{e}_1 - \boldsymbol{e}_2)^* & = & \mathrm{diag}(R_2R_3(c(2-3)+s(2+3)), \\ & & \quad R_1R_3(c(1-3)+s(1+3)), \\ & & \quad R_1R_2(c(1-2)+s(1+2))). \end{array} \tag{3.11}$$

The tensor $-\boldsymbol{E}(\theta_1, \theta_2)$ is diagonal, and positive if and only if $-E_{ii}(\theta_1, \theta_2) \geq 0$ for $i = 1, 2, 3$. Using (3.11), we obtain three inequalities of the form

$$R_jR_k[\theta_1\theta_2 s(j+k) + \theta_1(1-\theta_1)c_jc_k + \theta_2(1-\theta_2)s_js_k] \leq 0 \tag{3.12}$$

where $j \neq k$. We now show that the conditions (3.12) are actually equivalent to the requirements (3.9). Let us introduce the following matrix:

$$\Delta = \begin{pmatrix} s_1^2 & s_2^2 & s_3^2 \\ c_1^2 & c_2^2 & c_3^2 \\ -s_1c_1 & -s_2c_2 & -s_3c_3 \end{pmatrix}. \tag{3.13}$$

The condition (3.9) can be rewritten as

$$\Delta \begin{pmatrix} k_1 \\ k_2 \\ k_3 \end{pmatrix} = \begin{pmatrix} \theta_1(1-\theta_1) \\ \theta_2(1-\theta_2) \\ -\theta_1\theta_2 \end{pmatrix} \text{ with } k_r \geq 0. \tag{3.14}$$

Calculating the determinant of Δ gives $\det \Delta = s(3-2)s(1-2)s(1-3)$. By (3.4), the matrix Δ is thus invertible and the condition (3.9) is equivalent to

$$\Delta^{-1} \begin{pmatrix} \theta_1(1-\theta_1) \\ \theta_2(1-\theta_2) \\ -\theta_1\theta_2 \end{pmatrix} \geq 0. \tag{3.15}$$

The inversion of Δ yields

$$\Delta^{-1} = \frac{1}{\det \Delta} \begin{pmatrix} c_2c_3s(3-2) & s_2s_3s(3-2) & -s(3+2)s(3-2) \\ c_1c_3s(1-3) & s_1s_3s(1-3) & -s(1+3)s(1-3) \\ c_1c_2s(2-1) & s_1s_2s(2-1) & -s(1+2)s(2-1) \end{pmatrix}. \tag{3.16}$$

Substituting (3.16) in (3.15), we obtain the three following inequalities

$$\frac{1}{s(i-j)s(i-k)}[\theta_1\theta_2 s(j+k) + \theta_1(1-\theta_1)c_jc_k + \theta_2(1-\theta_2)s_js_k] \geq 0 \tag{3.17}$$

where $\{i,j,k\}$ is a permutation of $\{1,2,3\}$. Because of the condition (3.4), this inequality is equivalent to (3.12). Therefore, the upper bound $P\mathcal{K}$ coincides with $Q_{SW}\mathcal{K}$. It has to be emphasized that the mathematical arguments used by Smyshlyaev and Willis (namely a variational formulation of a Hashin–Shtrickman type) are of a different nature than those used for deriving the bound $P\mathcal{K}$.

4. Four-well problems

In this section, $\mathcal{K}$ is assumed to be of the form $\mathcal{K} = \{\boldsymbol{e}_1, \boldsymbol{e}_2, \boldsymbol{e}_3, \boldsymbol{e}_4\}$. The upper bound $P\mathcal{K}$ in (2.10) is compared with lower bounds resulting from sequential lamination techniques (Kohn, 1991). The construction of such lower bounds relies on the fact that if two given strains $\boldsymbol{e}$ and $\boldsymbol{e}'$ are compatible in the sense of (2.11), then any strain in the line segment $[\boldsymbol{e}, \boldsymbol{e}']$ is realized by a simple laminate. As mentioned earlier, the compatibility condition can be reformulated as $\lambda_2 = 0$, where $\lambda_1 \leq \lambda_2 \leq \lambda_3$ are the eigenvalues of $\boldsymbol{e} - \boldsymbol{e}'$. That condition can easily be proved to be equivalent to

$$\det(\boldsymbol{e} - \boldsymbol{e}') = 0, \tag{4.1}$$

$$(\mathrm{tr}(\boldsymbol{e} - \boldsymbol{e}'))^2 - (\boldsymbol{e} - \boldsymbol{e}') : (\boldsymbol{e} - \boldsymbol{e}') \leq 0. \tag{4.2}$$

Rank-r laminates can be constructed by using that argument in an iterative fashion. The set of strains realized by such laminates forms a lower bound on $Q\mathcal{K}$, denoted by $R_r\mathcal{K}$. We now detail a formal algorithm to construct $R_r\mathcal{K}$. That algorithm consists in determining a representation of $R_r\mathcal{K}$ in the form

$$R_r\mathcal{K} = \bigcup_{i \in I_r} [\boldsymbol{a}_r^i, \boldsymbol{b}_r^i] \tag{4.3}$$

where $\boldsymbol{a}_r^i$ and $\boldsymbol{b}_r^i$ are strains in $C\mathcal{K}$. Setting $R_0\mathcal{K}$ equal to $\mathcal{K}$, the set $R_{r+1}\mathcal{K}$ is constructed from $R_r\mathcal{K}$ by going through each pair of line segments $\{[\boldsymbol{a}_r^i, \boldsymbol{b}_r^i], [\boldsymbol{a}_r^j, \boldsymbol{b}_r^j]\}$ in (4.3) and looking for strains $\boldsymbol{e} \in [\boldsymbol{a}_r^i, \boldsymbol{b}_r^i]$ and $\boldsymbol{e}' \in [\boldsymbol{a}_r^j, \boldsymbol{b}_r^j]$ that are compatible. Writing $\boldsymbol{e}$ and $\boldsymbol{e}'$ as

$$\boldsymbol{e} = x\boldsymbol{a}_r^i + (1-x)\boldsymbol{b}_r^i \ , \ \boldsymbol{e}' = x'\boldsymbol{a}_r^j + (1-x')\boldsymbol{b}_r^j,$$

we need to solve the equation

$$0 = \det(\boldsymbol{e} - \boldsymbol{e}') = \det(x'(\boldsymbol{b}_r^j - \boldsymbol{a}_r^j) - x(\boldsymbol{b}_r^i - \boldsymbol{a}_r^i) + \boldsymbol{b}_r^i - \boldsymbol{b}_r^j). \tag{4.4}$$

That equation is a third-degree polynomial in (x, x'). For any root (x, x') in $[0,1] \times [0,1]$ verifying (4.2), the strains in the line segment $[\boldsymbol{e}, \boldsymbol{e}']$ are realized by rank-$(r+1)$ laminates of strains in $\mathcal{K}$. Taking the union of all such line segments gives the representation of $R_{r+1}\mathcal{K}$ in the form (4.3). That algorithm makes it clear that the dimension of the manifold $R_{r+1}\mathcal{K}$ (denoted by dim $R_{r+1}\mathcal{K}$) is bounded from above by $1 + \dim R_r\mathcal{K}$. It follows that

$$\dim R_r\mathcal{K} \leq r. \tag{4.5}$$

For $r > 1$, that algorithm may be difficult to execute by hand, but it can easily be implemented numerically. In that regard, a dramatic escalation in needed computational resources is observed as r increases. Computational time typically varies as M^r where M is a constant (depending on the size of $\mathcal{K}$). As a notable consequence, it proved difficult to get beyond $r = 3$ in the calculations. Also note that the above construction of lamination bounds is not restricted to four-well problems.

The different sets introduced so far satisfy the chain of inclusion

$$\mathcal{K} = R_0\mathcal{K} \subset R_1\mathcal{K} \subset \cdots \subset R_r\mathcal{K} \subset Q\mathcal{K} \subset P\mathcal{K} \subset C\mathcal{K} \subset \text{vect}(\mathcal{K})$$

where vect$(\mathcal{K})$ is the vectorial space spanned by $\mathcal{K}$. Since all those sets are included in vect$(\mathcal{K})$, the gap between two of them can be quantified by comparing their measures in vect$(\mathcal{K})$, as defined by

$$|\mathcal{S}| = \int_{\boldsymbol{e} \in \text{vect}(\mathcal{K})} \chi_{\mathcal{S}}(\boldsymbol{e}) d\boldsymbol{e} \tag{4.6}$$

where $\chi_{\mathcal{S}}$ is the characteristic function of the set $\mathcal{S}$ considered (i.e. $\chi_{\mathcal{S}}(\boldsymbol{e})$ is equal to 1 if $\boldsymbol{e} \in \mathcal{S}$, and null otherwise).

Consider the linear mapping f defined as

$$\begin{array}{rccl} f: & \mathbb{R}^3 & \to & \mathbb{R}^{3\times 3}_s \\ & (\theta_1, \theta_2, \theta_3) & \mapsto & \displaystyle\sum_{r=1}^{3} \theta_r \boldsymbol{e}_r + (1 - \sum_{r=1}^{3} \theta_r)\boldsymbol{e}_4. \end{array} \tag{4.7}$$

That mapping is injective if $\boldsymbol{e}_1 - \boldsymbol{e}_4$, $\boldsymbol{e}_2 - \boldsymbol{e}_4$, $\boldsymbol{e}_3 - \boldsymbol{e}_4$ are linearly independent, which is assumed from now on. The mapping f in (4.7) serves two purposes. First, since it defines a one-to-one mapping between $\mathbb{R}^3$ and $\mathbb{R}^{3\times 3}_s$, the mapping f provides 3-dimensional representations of the convex hull $\mathcal{K}$ and other

related bounds on $Q\mathcal{K}$. In particular, the convex hull $\mathcal{K}$ is represented by the tetrahedron $\mathcal{T}_3' = \{(\theta_1, \theta_2, \theta_3) \in \mathbb{R}^3_+ | \sum_{r=1}^3 \theta_r = 1\}$ and the upper bound $P\mathcal{K}$ is represented by the three-dimensional set $f^{-1}(P\mathcal{K})$ given by

$$f^{-1}(P\mathcal{K}) = \{\boldsymbol{\theta} \in \mathcal{T}_3' | 0 \leq -\sum_{r,s=1}^{3} \theta_r \theta_s (\boldsymbol{e}_r - \boldsymbol{e}_s)^* - 2(1 - \sum_{r=1}^{3} \theta_r) \sum_{s=1}^{3} \theta_s (\boldsymbol{e}_4 - \boldsymbol{e}_s)^*\}. \tag{4.8}$$

Second, the mapping f being affine, it allows for a simple calculation of measures in (4.6). We have indeed

$$|\mathcal{S}| = J \int_{\boldsymbol{\theta} \in f^{-1}(\mathcal{S})} d\theta \tag{4.9}$$

where J is the Jacobian of f and is equal to the mixed product $[\boldsymbol{e}_1 - \boldsymbol{e}_4, \boldsymbol{e}_2 - \boldsymbol{e}_4, \boldsymbol{e}_3 - \boldsymbol{e}_4]$. Since $f^{-1}(C\mathcal{K}) = \mathcal{T}_3'$ and $\int_{\boldsymbol{\theta} \in \mathcal{T}_3'} d\theta = 1/6$, we obtain

$$\frac{|\mathcal{S}|}{|C\mathcal{K}|} = 6 \int_{\boldsymbol{\theta} \in f^{-1}(\mathcal{S})} d\theta. \tag{4.10}$$

The ratio $|\mathcal{S}|/|C\mathcal{K}|$ is thus directly obtained from the volume of the three-dimensional set $f^{-1}(\mathcal{S})$. Note that $|C\mathcal{K}|$ and J are strictly positive if $\boldsymbol{e}_1 - \boldsymbol{e}_4$,$\boldsymbol{e}_2 - \boldsymbol{e}_4$,$\boldsymbol{e}_3 - \boldsymbol{e}_4$ are linearly independent. However, even in that case, it is generally not ensured that $|Q\mathcal{K}| > 0$.

4.1. Examples from the monoclinic-I transformation

The bounds detailed previously are now illustrated on some four-well problems related to the cubic to monoclinic-I transformation. There are 12 martensitic variants in that transformation, each variant being compatible with seven of the others (see Tables 1 and 2). In order to have a first insight in the structure of $Q\mathcal{K}^I$, we consider only four of the twelve transformations strains in Table 1. There are obviously a large number of four-well problems that can be constructed that way. The structure of the corresponding bounds is strongly dependent on the number of pairwise transformation strains in the four-well restriction that is considered. Rather than carrying out an exhaustive study of all the possibilities, we present a selection of examples which proves to be illustrative for our purpose, notably for the subsequent study of the twelve-well problem.

The first case we consider is $\mathcal{K}_4^I = \{\boldsymbol{e}_1^I, \boldsymbol{e}_2^I, \boldsymbol{e}_6^I, \boldsymbol{e}_{11}^I\}$. The three-dimensional set $f^{-1}(P\mathcal{K}_4^I)$ is represented in Figure 1 for Ti-49.75Ni. The values of the

$\boldsymbol{e}_1^I$	$\boldsymbol{e}_2^I$	$\boldsymbol{e}_3^I$	$\boldsymbol{e}_4^I$
$\begin{pmatrix} \alpha & \delta & \epsilon \\ \delta & \alpha & \epsilon \\ \epsilon & \epsilon & \beta \end{pmatrix}$	$\begin{pmatrix} \alpha & \delta & -\epsilon \\ \delta & \alpha & -\epsilon \\ -\epsilon & -\epsilon & \beta \end{pmatrix}$	$\begin{pmatrix} \alpha & -\delta & -\epsilon \\ -\delta & \alpha & \epsilon \\ -\epsilon & \epsilon & \beta \end{pmatrix}$	$\begin{pmatrix} \alpha & -\delta & \epsilon \\ -\delta & \alpha & -\epsilon \\ \epsilon & -\epsilon & \beta \end{pmatrix}$
$\boldsymbol{e}_5^I$	$\boldsymbol{e}_6^I$	$\boldsymbol{e}_7^I$	$\boldsymbol{e}_8^I$
$\begin{pmatrix} \alpha & \epsilon & \delta \\ \epsilon & \beta & \epsilon \\ \delta & \epsilon & \alpha \end{pmatrix}$	$\begin{pmatrix} \alpha & -\epsilon & \delta \\ -\epsilon & \beta & -\epsilon \\ \delta & -\epsilon & \alpha \end{pmatrix}$	$\begin{pmatrix} \alpha & -\epsilon & -\delta \\ -\epsilon & \beta & \epsilon \\ -\delta & \epsilon & \alpha \end{pmatrix}$	$\begin{pmatrix} \alpha & \epsilon & -\delta \\ \epsilon & \beta & -\epsilon \\ -\delta & -\epsilon & \alpha \end{pmatrix}$
$\boldsymbol{e}_9^I$	$\boldsymbol{e}_{10}^I$	$\boldsymbol{e}_{11}^I$	$\boldsymbol{e}_{12}^I$
$\begin{pmatrix} \beta & \epsilon & \epsilon \\ \epsilon & \alpha & \delta \\ \epsilon & \delta & \alpha \end{pmatrix}$	$\begin{pmatrix} \beta & -\epsilon & -\epsilon \\ -\epsilon & \alpha & \delta \\ -\epsilon & \delta & \alpha \end{pmatrix}$	$\begin{pmatrix} \beta & -\epsilon & \epsilon \\ -\epsilon & \alpha & -\delta \\ \epsilon & -\delta & \alpha \end{pmatrix}$	$\begin{pmatrix} \beta & \epsilon & -\epsilon \\ \epsilon & \alpha & -\delta \\ -\epsilon & -\delta & \alpha \end{pmatrix}$

Table 1: Transformation strains in the cubic to monoclinic-I transformation.

Variant	1	2	3	4	5	6	7	8	9	10	11	12
1	.	1	1	1	1	.	1	.	1	.	1	.
2	1	.	1	1	.	1	.	1	.	1	.	1
3	1	1	.	1	1	.	1	.	.	1	.	1
4	1	1	1	.	.	1	.	1	1	.	1	.
5	1	.	1	.	.	1	1	1	1	.	.	1
6	.	1	.	1	1	.	1	1	.	1	1	.
7	1	.	1	.	1	1	.	1	.	1	1	.
8	.	1	.	1	1	1	1	.	1	.	.	1
9	1	.	.	1	1	.	.	1	.	1	1	1
10	.	1	1	.	.	1	1	.	1	.	1	1
11	1	.	.	1	.	1	1	.	1	1	.	1
12	.	1	1	.	1	.	.	1	1	1	1	.

Table 2: Compatible variants (indicated by '1') in monoclinic-I martensite.

lattice parameters are $\alpha = 0.0243$, $\beta = -0.0437$, $\delta = 0.058$, $\epsilon = 0.0427$ (Knowles and Smith, 1981). In Figure 1 (top), two snapshots from different viewpoints are put together for a better grasp of the three-dimensional representation of $f^{-1}(P\mathcal{K}_4^I)$. Let us address a few comments on the shape of that set: since the pair $\{\boldsymbol{e}_1^I, \boldsymbol{e}_6^I\}$ is not compatible (see Table 2), any $\boldsymbol{\theta}$ in the line segment $]f^{-1}(\boldsymbol{e}_1^I), f^{-1}(\boldsymbol{e}_6^I)[$ is expected to be excluded from the set $f^{-1}(P\mathcal{K}_4^I)$. For such a value of $\boldsymbol{\theta}$, the tensor $-\sum_{r,s}\theta_r\theta_s(\boldsymbol{e}_r^I - \boldsymbol{e}_s^I)^*$ indeed reduces to $A(\boldsymbol{e}_1^I - \boldsymbol{e}_6^I)^*$ (with $A \neq 0$) and therefore is not positive. In a similar fashion, the pair $\{\boldsymbol{e}_2^I, \boldsymbol{e}_{11}^I\}$ is also incompatible, and the corresponding edge of the tetrahedron $\mathcal{T}_3'$ is expected to be excluded from $f^{-1}(P\mathcal{K}_4^I)$. As can be seen on Figure 1, there is actually a three-dimensional volume surrounding those two edges that is excluded from $f^{-1}(P\mathcal{K}_4^I)$. As a result, the measure of $P\mathcal{K}_4^I$ is smaller than the measure of the convex hull $C\mathcal{K}_4^I$: use of relation (4.10) gives $|P\mathcal{K}_4^I|/|C\mathcal{K}_4^I| \simeq 0.79$. The upper bound $P\mathcal{K}_4^I$ thus brings an significant improvement on the upper bound $C\mathcal{K}_4^I$.

One particular point of interest is to determine if the quasiconvex hull $Q\mathcal{K}_4^I$ has a non-empty interior, i.e. if $|Q\mathcal{K}_4^I|$ is strictly positive. Since $|R_n\mathcal{K}_4^I| < |Q\mathcal{K}_4^I|$, a sufficient condition is that $|R_n\mathcal{K}_4^I| > 0$ for some n. As as direct consequence of (4.5), it is necessary to take at least $n = 3$ for the corresponding set $R_n\mathcal{K}_4^I$ to have a non-empty interior. The set $R_3\mathcal{K}_4^I$ corresponding to rank-3 laminates is shown in Figure 1 (bottom). We find $|R_3\mathcal{K}_4^I|/|C\mathcal{K}_4^I| \simeq 0.6$, which confirms that $|Q\mathcal{K}_4^I|$ has a non-empty interior. Also observe that $R_3\mathcal{K}_4^I$ is found to have a similar shape as $P\mathcal{K}_4^I$. The gap between $R_3\mathcal{K}_4^I$ and $P\mathcal{K}_4^I$ is illustrated in Figure 2, on which those two sets are superimposed. The gap between $R_3\mathcal{K}_4^I$ and $P\mathcal{K}_4^I$ can be measured using relation (4.10), yielding $|R_3\mathcal{K}_4^I|/|P\mathcal{K}_4^I| \simeq 0.76$.

In Figure 3 is represented the upper bound $P\mathcal{K}_{4'}^I$ corresponding to $\mathcal{K}_{4'}^I = \{\boldsymbol{e}_1^I, \boldsymbol{e}_3^I, \boldsymbol{e}_6^I, \boldsymbol{e}_8^I\}$. In that case, only two of the six pairs of strains in $\mathcal{K}_{4'}^I$ are compatible (namely $\{\boldsymbol{e}_1^I, \boldsymbol{e}_3^I\}$ and $\{\boldsymbol{e}_6^I, \boldsymbol{e}_8^I\}$). Nevertheless, the set $P\mathcal{K}_{4'}^I$ is found to be quite close to the convex hull $C\mathcal{K}_{4'}^I$. As in the previous example, each edge connecting two incompatible strains is surrounded by a three-dimensional domain of strains that are not in $P\mathcal{K}_{4'}^I$. However, that domain is much smaller than in the previous example, resulting in a set $P\mathcal{K}_{4'}^I$ that is much closer to the convex hull. More precisely, we find using (4.10) that $|P\mathcal{K}_{4'}^I|/|C\mathcal{K}_{4'}^I| \simeq 0.94$. Consideration of the lower bound $R_3\mathcal{K}_4^I$ (not represented) leads to a similar conclusion (see Table 5).

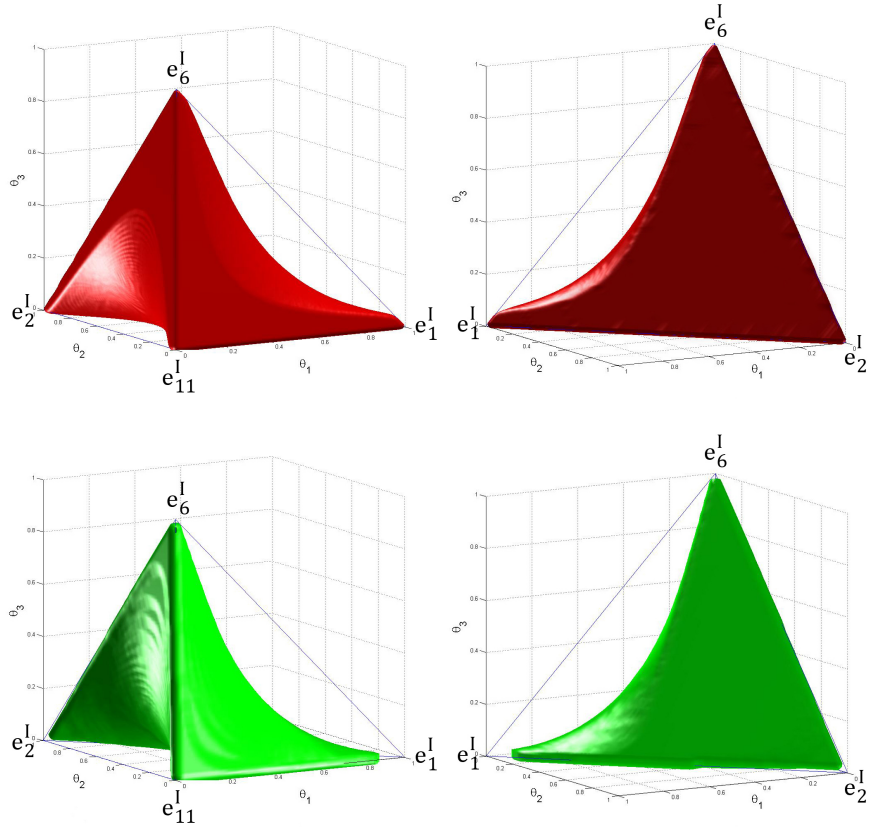

Figure 1: Three-dimensional representation of the upper bound $P\mathcal{K}_4^I$ (in red) and of the lower bound $R_3\mathcal{K}_4^I$ (in green).

4.2. Examples from the monoclinic-II transformation

We now examine some four-well problems related to monoclinic-II transformation. The 12 transformation strains of the cubic to monoclinic-II transformation are listed in Table 3. Each martensitic variant is compatible with seven of the others, just as for the cubic to monoclinic-I transformation (Table 4). We consider two examples of four-well problems that are the analogues of those studied previously for monoclinic-I martensite. Figure 4 shows the upper bound $P\mathcal{K}_4^{II}$ corresponding to $\mathcal{K}_4^{II} = \{\boldsymbol{e}_1^{II}, \boldsymbol{e}_2^{II}, \boldsymbol{e}_6^{II}, \boldsymbol{e}_{11}^{II}\}$. In a similar way to $\mathcal{K}_4^I$, $\{\boldsymbol{e}_1^{II}, \boldsymbol{e}_6^{II}\}$ and $\{\boldsymbol{e}_2^{II}, \boldsymbol{e}_{11}^{II}\}$ are the only pairs of strains in $\mathcal{K}_4^{II}$ that are not compatible. The set $P\mathcal{K}_4^{II}$ can be interpreted in a similar way as $P\mathcal{K}_4^I$, but the detailed shape of $f^{-1}(P\mathcal{K}_4^{II})$ is different from that of $f^{-1}(P\mathcal{K}_4^I)$ and

$\boldsymbol{e}_1^{II}$	$\boldsymbol{e}_2^{II}$	$\boldsymbol{e}_3^{II}$	$\boldsymbol{e}_4^{II}$
$\begin{pmatrix} \alpha+\epsilon & \delta & 0 \\ \delta & \alpha-\epsilon & 0 \\ 0 & 0 & \beta \end{pmatrix}$	$\begin{pmatrix} \alpha-\epsilon & \delta & 0 \\ \delta & \alpha+\epsilon & 0 \\ 0 & 0 & \beta \end{pmatrix}$	$\begin{pmatrix} \alpha+\epsilon & -\delta & 0 \\ -\delta & \alpha-\epsilon & 0 \\ 0 & 0 & \beta \end{pmatrix}$	$\begin{pmatrix} \alpha-\epsilon & -\delta & 0 \\ -\delta & \alpha+\epsilon & 0 \\ 0 & 0 & \beta \end{pmatrix}$
$\boldsymbol{e}_5^{II}$	$\boldsymbol{e}_6^{II}$	$\boldsymbol{e}_7^{II}$	$\boldsymbol{e}_8^{II}$
$\begin{pmatrix} \alpha+\epsilon & 0 & \delta \\ 0 & \beta & 0 \\ \delta & 0 & \alpha-\epsilon \end{pmatrix}$	$\begin{pmatrix} \alpha-\epsilon & 0 & \delta \\ 0 & \beta & 0 \\ \delta & 0 & \alpha+\epsilon \end{pmatrix}$	$\begin{pmatrix} \alpha+\epsilon & 0 & -\delta \\ 0 & \beta & 0 \\ -\delta & 0 & \alpha-\epsilon \end{pmatrix}$	$\begin{pmatrix} \alpha-\epsilon & 0 & -\delta \\ 0 & \beta & 0 \\ -\delta & 0 & \alpha+\epsilon \end{pmatrix}$
$\boldsymbol{e}_9^{II}$	$\boldsymbol{e}_{10}^{II}$	$\boldsymbol{e}_{11}^{II}$	$\boldsymbol{e}_{12}^{II}$
$\begin{pmatrix} \beta & 0 & 0 \\ 0 & \alpha-\epsilon & \delta \\ 0 & \delta & \alpha+\epsilon \end{pmatrix}$	$\begin{pmatrix} \beta & 0 & 0 \\ 0 & \alpha+\epsilon & \delta \\ 0 & \delta & \alpha-\epsilon \end{pmatrix}$	$\begin{pmatrix} \beta & 0 & 0 \\ 0 & \alpha-\epsilon & -\delta \\ 0 & -\delta & \alpha+\epsilon \end{pmatrix}$	$\begin{pmatrix} \beta & 0 & 0 \\ 0 & \alpha+\epsilon & -\delta \\ 0 & -\delta & \alpha-\epsilon \end{pmatrix}$

Table 3: Transformation strains in the cubic to monoclinic-II transformation.

Variant	1	2	3	4	5	6	7	8	9	10	11	12
1	.	1	1	1	1	.	1	.	1	.	1	.
2	1	.	1	1	.	1	.	1	.	1	.	1
3	1	1	.	1	1	.	1	.	1	.	1	.
4	1	1	1	.	.	1	.	1	.	1	.	1
5	1	.	1	.	.	1	1	1	.	1	.	1
6	.	1	.	1	1	.	1	1	1	.	1	.
7	1	.	1	.	1	1	.	1	.	1	.	1
8	.	1	.	1	1	1	1	.	1	.	1	.
9	1	.	1	.	.	1	.	1	.	1	1	1
10	.	1	.	1	1	.	1	.	1	.	1	1
11	1	.	1	.	.	1	.	1	1	1	.	1
12	.	1	.	1	1	.	1	.	1	1	1	.

Table 4: Compatible variants (indicated by the index '1') in monoclinic-II martensite.

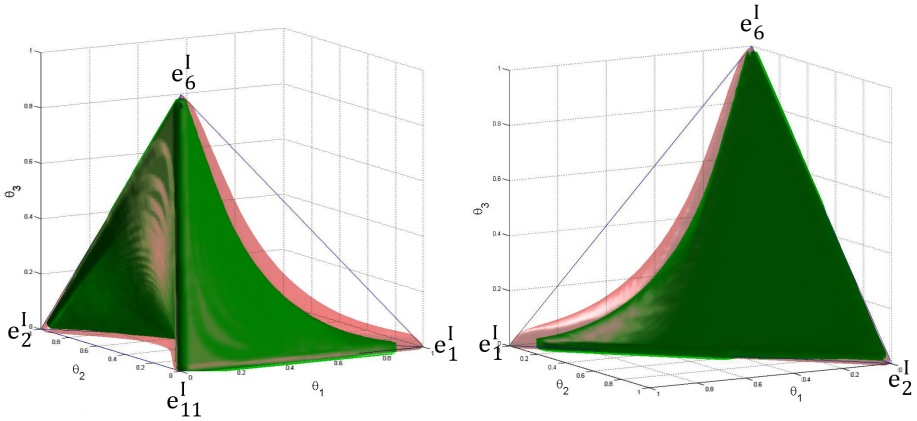

Figure 2: Three-dimensional representation of the upper bound $P\mathcal{K}_4^I$ with $\mathcal{K}_4^I = \{\boldsymbol{e}_1^I, \boldsymbol{e}_2^I, \boldsymbol{e}_6^I, \boldsymbol{e}_{11}^I\}$.

results in a smaller domain (see Table 5).

Let us now consider the quasiconvexification of $\mathcal{K}_{4'}^{II} = \{\boldsymbol{e}_1^{II}, \boldsymbol{e}_3^{II}, \boldsymbol{e}_6^{II}, \boldsymbol{e}_8^{II}\}$. The corresponding set $P\mathcal{K}_{4'}^{II}$ is represented on Figure 5. Even though the compatibility relations between the transformation strains in $\mathcal{K}_{4'}^{II}$ are the same as for $\mathcal{K}_{4'}^{I}$, the shape of $P\mathcal{K}_{4'}^{II}$ is dramatically different from that of $P\mathcal{K}_{4'}^{I}$. In particular, we can observe that $P\mathcal{K}_{4'}^{II}$ has two distinct connected components. It can be proved that one of these components is the line segment $[\boldsymbol{e}_6^{II}, \boldsymbol{e}_8^{II}]$ (see Appendix A). The other component is found to be a manifold of dimension 3 containing the line segment $[\boldsymbol{e}_1^{II}, \boldsymbol{e}_3^{II}]$. As can be guessed from Figure 5, the measure of $P\mathcal{K}_{4'}^{II}$ is very small: we find $|P\mathcal{K}_{4'}^{II}|/|C\mathcal{K}_{4'}^{II}| \simeq 0.006$. Concerning lower bounds, we find that $R_r\mathcal{K}_{4'}^{II} = [\boldsymbol{e}_1^{II}, \boldsymbol{e}_3^{II}] \cup [\boldsymbol{e}_6^{II}, \boldsymbol{e}_8^{II}]$ for $r \geq 1$. The reason is that no pair of compatible strains $\boldsymbol{e} \in [\boldsymbol{e}_1^{II}, \boldsymbol{e}_3^{II}]$ and $\boldsymbol{e}' \in [\boldsymbol{e}_6^{II}, \boldsymbol{e}_8^{II}]$ can be found.

Comparing those results with those obtained previously for monoclinic-I martensite (see Table 5), we observe that

$$\frac{|P\mathcal{K}_4^{II}|}{|C\mathcal{K}_4^{II}|} < \frac{|P\mathcal{K}_4^{I}|}{|C\mathcal{K}_4^{I}|}, \tag{4.11}$$

i.e. the set $P\mathcal{K}_4^I$ is closer to the convex hull $C\mathcal{K}_4^I$ than $P\mathcal{K}_4^{II}$ is to $C\mathcal{K}_4^{II}$. A

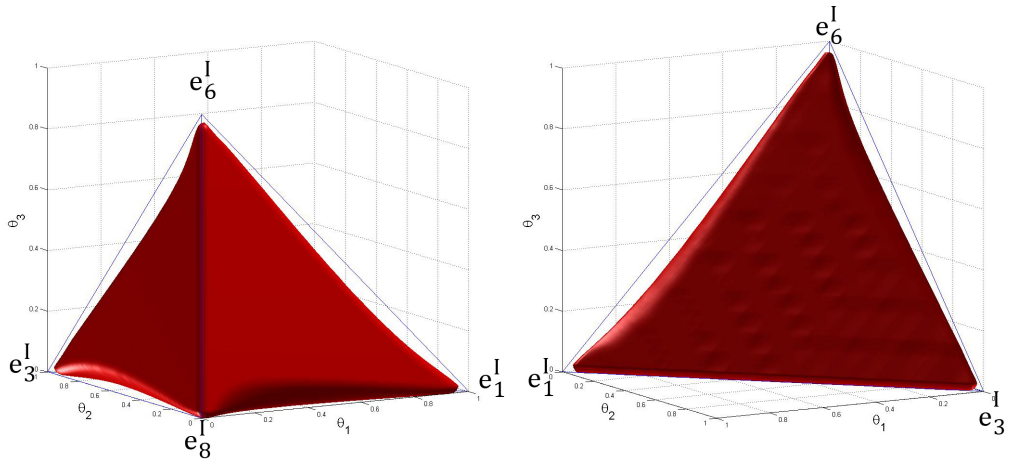

Figure 3: 3D representation of the upper bound $P\mathcal{K}^I_{4'}$ with $\mathcal{K}^I_{4'} = \{\boldsymbol{e}^I_1, \boldsymbol{e}^I_3, \boldsymbol{e}^I_6, \boldsymbol{e}^I_8\}$.

similar relation is verified by the lower bounds, i.e

$$\frac{|R_3\mathcal{K}^{II}_4|}{|C\mathcal{K}^{II}_4|} < \frac{|R_3\mathcal{K}^{I}_4|}{|C\mathcal{K}^{I}_4|}. \tag{4.12}$$

Analog inequalities are obtained between $\mathcal{K}^I_{4'}$ and $\mathcal{K}^{II}_{4'}$:

$$\frac{|R_3\mathcal{K}^{II}_{4'}|}{|C\mathcal{K}^{II}_{4'}|} < \frac{|R_3\mathcal{K}^{I}_{4'}|}{|C\mathcal{K}^{I}_{4'}|} \text{ and } \frac{|P\mathcal{K}^{II}_{4'}|}{|C\mathcal{K}^{II}_{4'}|} < \frac{|P\mathcal{K}^{I}_{4'}|}{|C\mathcal{K}^{I}_{4'}|}.$$

Morever, $|P\mathcal{K}^{II}_{4'}|/|C\mathcal{K}^{II}_{4'}| < |R_3\mathcal{K}^{I}_{4'}|/|C\mathcal{K}^{I}_{4'}|$ so that

$$\frac{|Q\mathcal{K}^{II}_{4'}|}{|C\mathcal{K}^{II}_{4'}|} < \frac{|Q\mathcal{K}^{I}_{4'}|}{|C\mathcal{K}^{I}_{4'}|}. \tag{4.13}$$

That inequality shows that the quasiconvexhull $Q\mathcal{K}^I_{4'}$ is closer to $C\mathcal{K}^I_{4'}$ than $Q\mathcal{K}^{II}_{4'}$ is to $C\mathcal{K}^{II}_{4'}$. The relations (4.11)-(4.12) suggest that a property similar to (4.13) also holds between $\mathcal{K}^I_4$ and $\mathcal{K}^{II}_4$, although this can not be proved rigorously from (4.11)-(4.12).

5. Twelve-well problems in monoclinic martensite

5.1. Convex bounds

In this Section we study the quasiconvexification of the sets $\mathcal{K}^I = \cup_{r=1}^{12}\{\boldsymbol{e}^I_r\}$ and $\mathcal{K}^{II} = \cup_{r=1}^{12}\{\boldsymbol{e}^{II}_r\}$, thus considering the 12 transformation strains in the

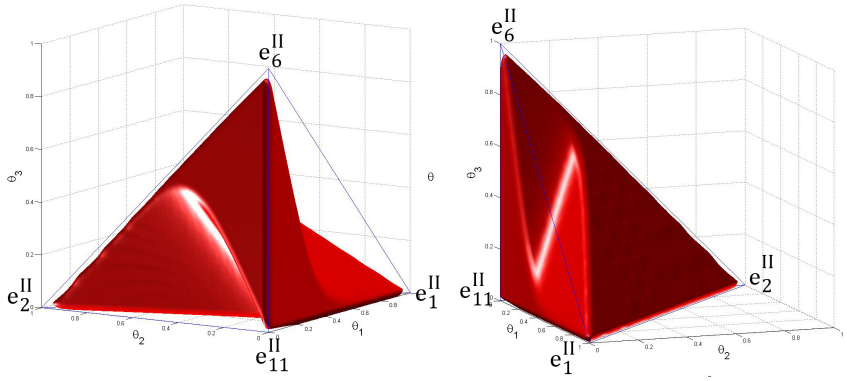

Figure 4: 3D representation of the upper bound $P\mathcal{K}_4^{II}$ with $\mathcal{K}_4^{II} = \{\boldsymbol{e}_1^{II}, \boldsymbol{e}_2^{II}, \boldsymbol{e}_6^{II}, \boldsymbol{e}_{11}^{II}\}$.

$\mathcal{K}$	$\lvert R_3\mathcal{K}\rvert/\lvert C\mathcal{K}\rvert$	$\lvert P\mathcal{K}\rvert/\lvert C\mathcal{K}\rvert$
Monoclinic-I		
Variants 1,2,6,11	0.60	0.79
Variants 1,3,6,8	0.82	0.94
Monoclinic-II		
Variants 1,2,6,11	0.57	0.65
Variants 1,3,6,8	0	0.006

Table 5: Measures of the bounding sets (expressed as fractions of $|C\mathcal{K}|$) for some 4-well problems related to monoclinic martensite.

two types of cubic to monoclinic transformations.

Bhattacharya and Kohn (1997) proved that the set $Q\mathcal{K}^I$ is not convex, and conjectured that a similar property holds for monoclinic-II martensite. Such a property does not follow directly from the fact that the set $P\mathcal{K}_{4'}^{II}$ represented in Figure 5 is non-convex : the family $(\boldsymbol{e}_1^{II}, \cdots, \boldsymbol{e}_{12}^{II})$ being not free, the decomposition

$$\bar{\boldsymbol{e}} = \sum_{r=1}^{12} \theta_r \boldsymbol{e}_r^{II} \tag{5.1}$$

of a given tensor $\bar{\boldsymbol{e}}$ is generally not unique. However, consider the intersection of the convex hull $C\mathcal{K}^{II}$ with the subspace H defined by the equations $\bar{e}_{12} = \bar{e}_{13} = \delta/2$, assuming that $\delta > 0$ (the variants in Table 3 can always be numbered in such a way that this condition is satisfied). For any $\bar{\boldsymbol{e}}$ in $C\mathcal{K}^{II} \cap$

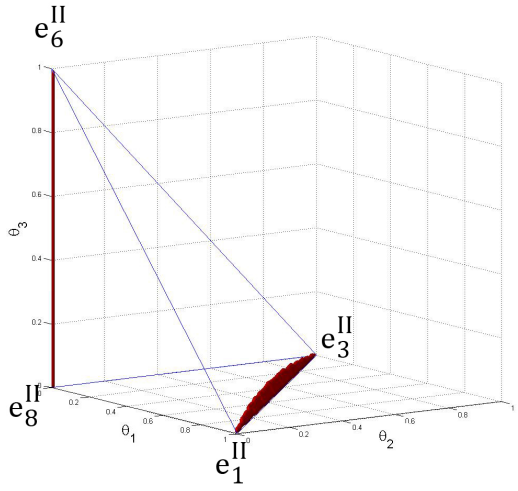

Figure 5: 3D representation of the upper bound $P\mathcal{K}_4^{II}$ with $\mathcal{K}_4^{II} = \{\boldsymbol{e}_1^{II}, \boldsymbol{e}_3^{II}, \boldsymbol{e}_6^{II}, \boldsymbol{e}_8^{II}\}$.

H, the decomposition (5.1) is unique and satisfies

$$\theta_1 + \theta_2 = \theta_5 + \theta_6 = \frac{1}{2}. \tag{5.2}$$

Let us briefly justify this assertion. For a fixed $\bar{\boldsymbol{e}}$ in $C\mathcal{K}^{II} \cap H$, there exists $\boldsymbol{\theta}$ in $\mathcal{T}_{12}$ such that $\bar{\boldsymbol{e}} = \sum_{r=1}^{12} \theta_r \boldsymbol{e}_r^{II}$. Using Table 3, we have $\bar{e}_{12} = \delta(\theta_1 + \theta_2 - \theta_3 - \theta_4) \leq \delta(\theta_1 + \theta_2)$. In a similar fashion, we have $\bar{e}_{13} \leq (\theta_5 + \theta_6)\delta$. Therefore, the equations $\bar{e}_{12} = \bar{e}_{13} = \delta/2$ imply that $1/2 \leq \theta_1 + \theta_2$ and $1/2 \leq \theta_5 + \theta_6$. Since $\boldsymbol{\theta} \in \mathcal{T}_{12}$, these conditions can be realized only if $1/2 = \theta_1 + \theta_2 = \theta_5 + \theta_6$ and $\theta_r = 0$ for $r \notin \{1, 2, 5, 6\}$. The decomposition (5.2) is thus obtained. The uniqueness of this decomposition comes from the fact that the tensors $(\boldsymbol{e}_1^{II}, \boldsymbol{e}_2^{II}, \boldsymbol{e}_3^{II}, \boldsymbol{e}_4^{II})$ in Table 3 are linearly independent.

Consider now the tensor $(\boldsymbol{e}_1^{II} + \boldsymbol{e}_6^{II})/2$, which is in $C\mathcal{K}^{II} \cap H$. It can be easily verified that $-(\boldsymbol{e}_1^{II} - \boldsymbol{e}_6^{II})^*$ is not positive. Since the decomposition (5.1) is unique, it can be concluded from (2.10) that $(\boldsymbol{e}_1^{II} + \boldsymbol{e}_6^{II})/2$ is excluded from $P\mathcal{K}^{II}$, and a fortiori from $Q\mathcal{K}^{II}$. This proves that $Q\mathcal{K}^{II}$ is not convex.

From here onwards we use the notation $\mathcal{K}$ to denote indifferently $\mathcal{K}^I$ or $\mathcal{K}^{II}$. The corresponding transformations strains are denoted by $\boldsymbol{e}_r$ (i.e. $\boldsymbol{e}_r = \boldsymbol{e}_r^I$ for $\mathcal{K} = \mathcal{K}^I$, and $\boldsymbol{e}_r = \boldsymbol{e}_r^{II}$ for $\mathcal{K} = \mathcal{K}^{II}$). In the literature so far, the structure of $Q\mathcal{K}$ in cubic to monoclinic transformations has been essentially

studied using convex bounds. Since $Q\mathcal{K}$ is not convex, such bounds can only be *strict*. Shu and Bhattacharya (1998) notably used the convex hull of $C\mathcal{K}$ to bound $Q\mathcal{K}$ from above. A convex lower bound has been proposed in closed form by Bhattacharya and Kohn (1997). Noting that $\boldsymbol{e}_{2i-1}$ and $\boldsymbol{e}_{2i}$ are compatible for each $i = 1, \cdots, 6$ (see Tables 2-4), Bhattacharya and Kohn (1997) observed that $Q\mathcal{K}$ contains the strains $\boldsymbol{e}'_i = (\boldsymbol{e}_{2i-1}+\boldsymbol{e}_{2i})/2$. The strains $\boldsymbol{e}'_1, \cdots, \boldsymbol{e}'_6$ can be verified to be pairwise compatible (they actually correspond to the six transformation strains of the cubic to orthorombic transformation). As a consequence, $Q\mathcal{K}$ contains the convex hull $\mathcal{S}$ of $\boldsymbol{e}'_1, \cdots, \boldsymbol{e}'_6$. As proved by Bhattacharya and Kohn (1997), the set $\mathcal{S}$ is formed by the tensors $\bar{\boldsymbol{e}}$ satisfying the conditions:

$$\begin{gathered} \operatorname{tr} \bar{\boldsymbol{e}} = 2\alpha + \beta; \\ \min(\alpha, \beta) \leq \bar{e}_{ii} \leq \max(\alpha, \beta) \text{ for i=1, 2, 3;} \\ |\bar{e}_{jk}| \leq \frac{\bar{e}_{ii} - \alpha}{\beta - \alpha}\delta \text{ for all } \{i, j, k\} \text{ permutation of } \{1, 2, 3\}. \end{gathered} \tag{5.3}$$

It can be proved that $\mathcal{S}$ has a non-empty interior in the 5-dimensional space $\{\bar{\boldsymbol{e}} | tr\bar{\boldsymbol{e}} = 2\alpha + \beta\}$ (Bhattacharya and Kohn, 1997). Consequently, $Q\mathcal{K}$ is of dimension 5, contrary to the four variant cases considered in Section 4 for which the sets $Q\mathcal{K}_4^I$ and $Q\mathcal{K}_4^{II}$ are manifolds of dimension 3.

A schematic representation of the convex bounds $\mathcal{S}$ and $C\mathcal{K}$ is given in Figure 6. In that Figure, the 12 transformation strains are represented as cocyclic points. Compatible transformation strains are connected by a line segment (for simplicity, each transformation strain is represented as being compatible with only two of the others). The lower bound $\mathcal{S}$ (shown in green) is constructed as the convex hull of six particular points (which are middle points of line segments connecting compatible transformation strains). The upper bound $C\mathcal{K}$ is the union of the red and green domains.

The gap between the convex bounds $\mathcal{S}$ and $C\mathcal{K}$ can be quantified by comparing the measures of those two sets. Those measures are defined as in (4.6), except that $\operatorname{vect}\mathcal{K}$ is now the $5-$dimensional space $\{\bar{\boldsymbol{e}} | \operatorname{tr} \bar{\boldsymbol{e}} = 2\alpha + \beta\}$. As mentioned above, the set $\mathcal{S}$ has a non-empty interior in $\operatorname{vect}\mathcal{K}$ and therefore has a non-zero measure. The exact value of $|\mathcal{S}|$ can be calculated from the analytical expression (5.3) of $\mathcal{S}$. In lack of a closed-form expression of $C\mathcal{K}$, its measure is obtained numerically using the algorithm of Barber et al. (1996) for calculating convex hulls in vectorial spaces of arbitrary dimension. The calculations of $|\mathcal{S}|$ and $|C\mathcal{K}|$ have been performed for several materials, using measurements of lattice parameters from the literature (Knowles

and Smith, 1981; Seo and Schryvers, 1998; Saburi et al., 1976; Tadaki et al., 1975; Chakravorty and Wayman, 1977). Corresponding values of the ratio $|\mathcal{S}|/|C\mathcal{K}|$ are reported in the first column of Table 6. As can be observed in that table, the ratio $|\mathcal{S}|/|C\mathcal{K}|$ is relatively low (< 0.18) in all the examples considered, especially in the case of monoclinic-I martensite for which it does not exceed 0.07. This is an indication that the gap between the two bounds $\mathcal{S}$ and $C\mathcal{K}$ is relatively large. In the following, we aim at refining our knowledge of $Q\mathcal{K}$ by deriving tighter bounds.

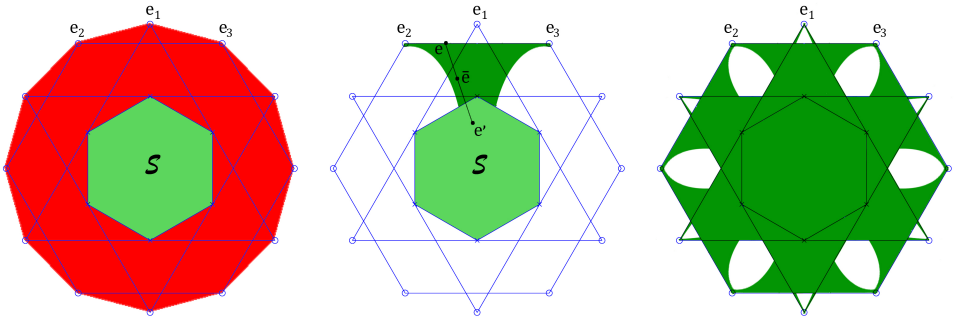

Figure 6: Schematic representations of the convex bounds (left) and of the lower bound $S_1\mathcal{K}$ (right) for monoclinic martensite. The line segments form the set $R_1\mathcal{K}$. The lower bound $S_1\mathcal{K}$ is constructed by looking for strains $\bar{\boldsymbol{e}}$ that are realized by simple lamination of a strain $\boldsymbol{e}'$ in $\mathcal{S}$ and a strain $\boldsymbol{e}$ on a line segment in $R_1\mathcal{K}$, such as $[\boldsymbol{e}_2, \boldsymbol{e}_3]$ (middle).

5.2. Non-convex bounds

In this section, we investigate the structure of $Q\mathcal{K}$ by deriving non-convex upper bounds and lower bounds similar in nature to those considered previously for the four-well problem. The consideration of the 12 variants, however, add some complication in the derivation of those bounds. Concerning the upper bound $P\mathcal{K}$, the main difficulty is that the decomposition of a strain $\bar{\boldsymbol{e}}$ in the form

$$\bar{\boldsymbol{e}} = \sum_{r=1}^{12} \theta_r \boldsymbol{e}_r \tag{5.4}$$

is not unique. More precisely, consider the mapping g defined as

$$\begin{array}{rccc} g: & \mathbb{R}^{12} & \to & \mathbb{R}^{3\times 3}_s \\ & (\theta_1, \cdots, \theta_{12}) & \mapsto & \displaystyle\sum_{r=1}^{12} \theta_r \boldsymbol{e}_r. \end{array} \tag{5.5}$$

Except for special values of the lattice parameters, $\operatorname{Ker} g$ is a vectorial space of dimension 7. Denoting by $\tilde{g}$ the (injective) restriction of g on $(\operatorname{Ker} g)^{\perp}$, the set of solutions to (5.4) is the affine space defined as

$$g^{-1}(\bar{\boldsymbol{e}}) = \tilde{g}^{-1}(\bar{\boldsymbol{e}}) + \operatorname{Ker} g. \tag{5.6}$$

Let $\mathcal{A}$ be the bounded subset of $\mathbb{R}^{12}$ defined as

$$\mathcal{A} = \{\boldsymbol{\theta} \in \mathcal{T}_{12} | - \sum_{r,s} \theta_r \theta_s (\boldsymbol{e}_r - \boldsymbol{e}_s)^* \geq 0\}.$$

From (2.10), the distinctive property of strains $\bar{\boldsymbol{e}}$ in $P\mathcal{K}$ is

$$g^{-1}(\bar{\boldsymbol{e}}) \cap \mathcal{A} \neq \emptyset. \tag{5.7}$$

Assuming that $\bar{\boldsymbol{e}}$ is given and using a numerical approach, it is relatively easy to determine if (5.7) is satisfied or not.

Difficulties in deriving meaningful non-convex lower bounds are more substantial. It has already be mentioned that $Q\mathcal{K}$ has a non-empty interior, i.e. that $|Q\mathcal{K}| > 0$. The relation (4.5) shows that it is necessary to take at least $r = 5$ for the corresponding bound $R_r\mathcal{K}$ to have a non-zero measure. However, for twelve-well problems, it proves difficult to get beyond $r = 2$ in the numerical calculations. Note that rank-2 laminates have been considered by Govindjee et al. (2007) for bounding the effective energy in cubic to monoclinic transformations.

An alternative approach which proves to be fruitful is to consider simple laminates involving compatible strains in $\mathcal{S}$ and $R_r\mathcal{K}$, i.e. to consider the set $S_r\mathcal{K}$ defined as

$$S_r\mathcal{K} = \bigcup_{\substack{\boldsymbol{e}\in R_r\mathcal{K}, \boldsymbol{e}'\in\mathcal{S} \\ \det(\boldsymbol{e}-\boldsymbol{e}')=0}} [\boldsymbol{e}, \boldsymbol{e}']. \tag{5.8}$$

That set is a lower bound on $Q\mathcal{K}$ and contains $\mathcal{S}$ for $r \geq 1$. The motivation for introducing the set $S_r\mathcal{K}$ in (5.8) is that, contrary to $R_r\mathcal{K}$, it has a non-zero measure for any $r \geq 1$. In particular, we can use values of r that are

low enough for the computations to remain tractable (typically $r \leq 2$). The expectation - which remains to be confirmed at that point - is that $S_r\mathcal{K}$ is strictly larger than $R_r\mathcal{K} \cup \mathcal{S}$.

The following property, illustrated in Figure 6 (middle), is easily proved from (5.8):

A given strain $\bar{\boldsymbol{e}}$ is in $S_r\mathcal{K}$ if there exists a strain $\boldsymbol{e} \in R_r\mathcal{K}$ such that :
(i) $\boldsymbol{e}$ is compatible with $\bar{\boldsymbol{e}}$,
(ii) the half line $\{\boldsymbol{e} + y(\bar{\boldsymbol{e}} - \boldsymbol{e}) | y \geq 0\}$ intersects $\mathcal{S}$.
(5.9)

That characterization of $S_r\mathcal{K}$ is well suited to numerical implementation. Assume indeed that the decomposition (4.3) of $R_r\mathcal{K}$ is known (using for instance the algorithm detailed in Section 4). To test if a given strain $\bar{\boldsymbol{e}}$ is in $S_r\mathcal{K}$, we can go through each line segment $[\boldsymbol{a}_i^r, \boldsymbol{b}_i^r]$ in (4.3) and look for strains $\boldsymbol{e} = x\boldsymbol{a}_i^r + (1-x)\boldsymbol{b}_i^r$ that are compatible with $\bar{\boldsymbol{e}}$. Corresponding values of $x \in [0, 1]$ are roots of the 3rd-degree polynom $\det(x\boldsymbol{a}_i^r + (1-x)\boldsymbol{b}_i^r - \bar{\boldsymbol{e}})$. For any such $\boldsymbol{e}$, we can use the relations (5.3) to determine if $\mathcal{S}$ has a non-empty intersection with the half-line $\{\boldsymbol{e} + y(\bar{\boldsymbol{e}} - \boldsymbol{e}) | y \geq 0\}$. If this is the case, then the strain $\bar{\boldsymbol{e}}$ considered is in $S_r\mathcal{K}$.

5.3. Examples

In order to quantify the improvement brought upon by the bounds $S_r\mathcal{K}$ and $P\mathcal{K}$, we first calculate their measures and compare the results to the measures of $\mathcal{S}$ and $C\mathcal{K}$. A Monte-Carlo method is used to evaluate the integrals (4.6) that define $|S_r\mathcal{K}|$ and $|P\mathcal{K}|$. In those integrals, the functions $\chi_{P\mathcal{K}}(\bar{\boldsymbol{e}})$ and $\chi_{S_r\mathcal{K}}(\bar{\boldsymbol{e}})$ are calculated using the characterizations (5.7) and (5.9). Table 6 shows the results obtained for several materials, both for monoclinic-I and monoclinic-II martensite.

A first observation is that in all cases, the lower bounds $S_r\mathcal{K}$ dramatically improve on the convex lower bound $\mathcal{S}$. The upper bound $P\mathcal{K}$ significantly improves on $C\mathcal{K}$ for monoclinic-II martensite, but remains close to $C\mathcal{K}$ for monoclinic-I martensite (in a similar way to the four-well example $\mathcal{K}_{4'}^I$ of Section 4.1). As a corollary, the gap between the best available bounds (namely $S_2\mathcal{K}$ and $P\mathcal{K}$) is greatly reduced compared to the gap between the convex bounds ($\mathcal{S}$ and $C\mathcal{K}$), yielding a much improved estimate of $Q\mathcal{K}$. Comparing the results for monoclinic-I martensite with those for monoclinic-

	$\lvert\mathcal{S}\rvert/\lvert C\mathcal{K}\rvert$	$\lvert S_1\mathcal{K}\rvert/\lvert C\mathcal{K}\rvert$	$\lvert S_2\mathcal{K}\rvert/\lvert C\mathcal{K}\rvert$	$\lvert P\mathcal{K}\rvert/\lvert C\mathcal{K}\rvert$
Monoclinic-I				
Ni-49.75Ti	0.0645	0.543	0.824	0.994
CuZr	0.0543	0.547	0.865	0.998
Monoclinic-II				
Cu-20Zn-12Ga	0.154	0.576	0.787	0.922
Cu-39.3Zn	0.131	0.539	0.761	0.924
Cu-15Zn-17Al	0.176	0.592	0.756	0.917
β_1' Cu-14Al-4Ni	0.0915	0.470	0.706	0.918

Table 6: Measures of the bounding sets (expressed as fractions of $|C\mathcal{K}|$).

II martensite, we observe that

$$\frac{|P\mathcal{K}^I|}{|C\mathcal{K}^I|} < \frac{|P\mathcal{K}^{II}|}{|C\mathcal{K}^{II}|},$$

i.e. the set $P\mathcal{K}^I$ is thus closer to the convex hull $C\mathcal{K}^I$ than the set $P\mathcal{K}^{II}$ is to the set $C\mathcal{K}^{II}$. The best available lower bound $S_2\mathcal{K}$ satisfies the same property, that is to say

$$\frac{|S_2\mathcal{K}^I|}{|C\mathcal{K}^I|} < \frac{|S_2\mathcal{K}^{II}|}{|C\mathcal{K}^{II}|}.$$

That situation is reminiscent of the four-well examples presented in Section 4, for which similar relations were observed. This might be an indication that the set $Q\mathcal{K}^I$ is closer to its corresponding convex hull than the set $Q\mathcal{K}^{II}$.

Although calculating measures is instructive in getting a global picture, it does not fully characterize the various bounding sets introduced, nor the estimate of $Q\mathcal{K}$ that results from those bounds: the gap between $S_2\mathcal{K}$ and $P\mathcal{K}$ is typically expected to be larger in certain directions than in others. To better illustrate that point, we consider effective strains $\bar{\boldsymbol{e}}(\omega, \tau)$ of the form

$$\bar{\boldsymbol{e}}(\omega, \tau) = \frac{1}{3}(2\alpha + \beta)\boldsymbol{I} + \tau(\boldsymbol{u}(\omega) \otimes \boldsymbol{v}(\omega) + \boldsymbol{v}(\omega) \otimes \boldsymbol{u}(\omega)), \tag{5.10}$$

with

$$\boldsymbol{u}(\omega) = \cos(\omega)\boldsymbol{u}_1 + \sin(\omega)\boldsymbol{u}_2 \ , \ \boldsymbol{v}(\omega) = -\sin(\omega)\boldsymbol{u}_1 + \cos(\omega)\boldsymbol{u}_2.$$

In those expressions, $(\boldsymbol{u}_1, \boldsymbol{u}_2, \boldsymbol{u}_3)$ is an orthonormal basis of the cubic austenitic lattice. For latter reference, note that the matrix representation of $\bar{\boldsymbol{e}}(\omega, \tau)$

in the basis $(\boldsymbol{u}_1, \boldsymbol{u}_2, \boldsymbol{u}_3)$ is

$$\bar{\boldsymbol{e}}(\omega, \tau) = \frac{2\alpha + \beta}{3}\boldsymbol{I} + \tau \begin{pmatrix} -\sin 2\omega & \cos 2\omega & 0 \\ \cos 2\omega & \sin 2\omega & 0 \\ 0 & 0 & 0 \end{pmatrix}. \tag{5.11}$$

The strain $\bar{\boldsymbol{e}}(\omega, \tau)$ can be achieved by cooling down a stress-free sample below the transformation temperature and subsequently applying a simple shear of amplitude 2τ (between the directions $\boldsymbol{u}(\omega)$ and $\boldsymbol{v}(\omega)$) in the cooled state. Cooling down a stree-free sample indeed produces the so-called self-accommodated state in which there is no austenite and all the martensitic variants appear in equal volume fraction, resulting in a macroscopic strain $(2\alpha + \beta)/3\boldsymbol{I}$. We are interested in bounding the values of (ω, τ) for which $\bar{\boldsymbol{e}}(\omega, \tau) \in Q\mathcal{K}$. As monoclinic martensite is invariant in the $\boldsymbol{u}_1 \mapsto -\boldsymbol{u}_1$ symmetry, the conditions $\bar{\boldsymbol{e}}(\omega, \tau) \in Q\mathcal{K}$ and $\bar{\boldsymbol{e}}(\omega, -\tau) \in Q\mathcal{K}$ are equivalent. It is therefore sufficient to consider only positive values of τ. Let

$$S\tau(\omega) = \sup\{\tau | \bar{\boldsymbol{e}}(\omega, \tau) \in \mathcal{S}\}.$$

Since $\mathcal{S}$ is convex and closed, we have $\bar{\boldsymbol{e}}(\omega, \tau) \in \mathcal{S}$ for any positive τ such that $\tau \leq S\tau(\omega)$. It can be calculated from (5.3) that

$$S\tau(\omega) = \min\left(\frac{A}{|\sin 2\omega|}, \frac{\delta}{3|\cos 2\omega|}\right) \tag{5.12}$$

where

$$A = \min\left(\frac{2\alpha + \beta}{3} - \min(\alpha, \beta), -\frac{2\alpha + \beta}{3} + \max(\alpha, \beta)\right).$$

In a similar fashion, we define

$$\begin{array}{lll} C\tau(\omega) = \sup\{\tau | \bar{\boldsymbol{e}}(\omega, \tau) \in C\mathcal{K}\} & , & Q\tau(\omega) = \sup\{\tau | \bar{\boldsymbol{e}}(\omega, \tau) \in Q\mathcal{K}\}, \\ P\tau(\omega) = \sup\{\tau | \bar{\boldsymbol{e}}(\omega, \tau) \in P\mathcal{K}\} & , & S_r\tau(\omega) = \sup\{\tau | \bar{\boldsymbol{e}}(\omega, \tau) \in S_r\mathcal{K}\}. \end{array}$$

The relations $\mathcal{S} \subset S_1\mathcal{K} \subset S_2\mathcal{K} \subset Q\mathcal{K} \subset P\mathcal{K} \subset C\mathcal{K}$ imply that

$$S\tau \leq S_1\tau \leq S_2\tau \leq Q\tau \leq P\tau \leq C\tau. \tag{5.13}$$

Since $C\mathcal{K}$ is convex and closed, we have $\bar{\boldsymbol{e}}(\omega, \tau) \in C\mathcal{K}$ for any $0 \leq \tau \leq C\tau(\omega)$. Even though $P\mathcal{K}$ and $S_r\mathcal{K}$ are not convex, numerical computations show that they satisfy a similar property, i.e. $\bar{\boldsymbol{e}}(\omega, \tau) \in P\mathcal{K}$ for any $0 \leq \tau \leq P\tau(\omega)$, and $\bar{\boldsymbol{e}}(\omega, \tau) \in S_r\mathcal{K}$ for any $0 \leq \tau \leq S_r\tau(\omega)$. The functions $S\tau$, $S_r\tau$, $P\tau$ and

$C\tau$ thus completely characterize the intersection of the various bounding sets with strains of the form (5.10). Those functions are represented in Figure 7 for Ni-49.75Ti (monoclinic-I martensite) and in Figure 8 for β_1'Cu-14Al-4Ni (monoclinic-II martensite). It is obvious from the definition (5.10) that all those functions are of period π. As can be observed in Figures 7-8, they are also invariant in the $\omega \mapsto \pi/2 - \omega$ and $\omega \mapsto \pi - \omega$ symmetries. This can be verified to stem from the invariance of monoclinic martensite in the $(\boldsymbol{u}_1, \boldsymbol{u}_2) \mapsto (\boldsymbol{u}_2, \boldsymbol{u}_1)$ and $\boldsymbol{u}_2 \mapsto -\boldsymbol{u}_2$ transformations, respectively. Let us now study the results of Figures 7-8 in more detail. Because of the mentioned symmetries, we limit our attention to $\omega \in [0, \pi/4]$.

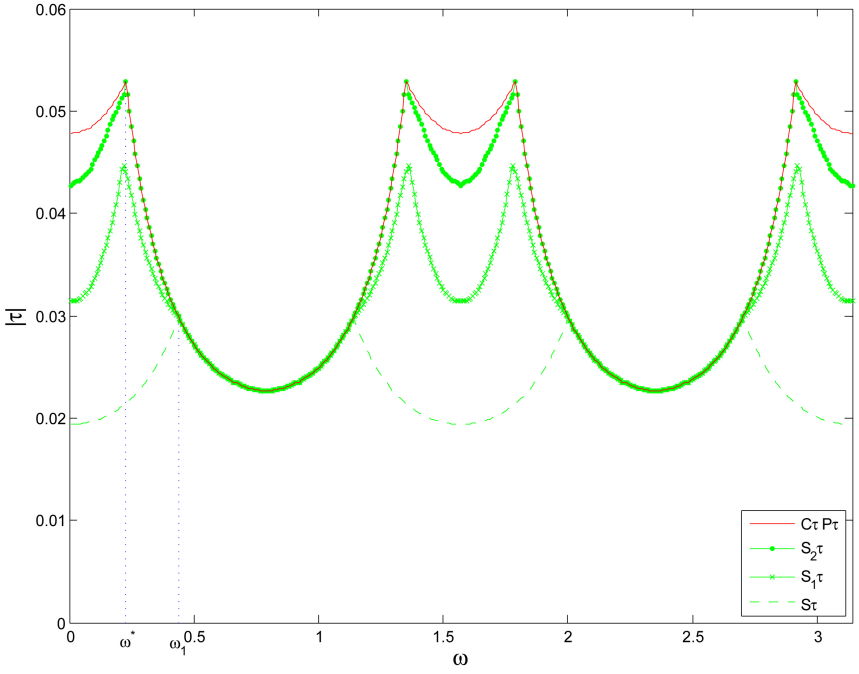

Figure 7: Bounds on (ω, τ) such that $\bar{\boldsymbol{e}}(\omega, \tau) \in Q\mathcal{K}^I$.

Concerning the monoclinic-I example (Figure 7), it can be proved that $S\tau$ coincides with $C\tau$ on an interval of the form $[\omega_1, \pi/4]$. The value of ω_1 is given by

$$\tan 2\omega_1 = \frac{\alpha - \beta}{\delta}.$$

Indeed, for $\omega_1 \leq \omega \leq \pi/4$, it can easily be calculated that $A/|\sin 2\omega|$ reaches the minimum in (5.12). Use of (5.11) gives

$$\bar{e}_{22}(\omega, S\tau(\omega)) = \max(\alpha, \beta).$$

Note that any $\bar{\boldsymbol{e}} \in C\mathcal{K}^I$ satisfies

$$\max_{i=1,2} \bar{e}_{ii} \leq \max_r e^I_{r,12} = \max(\alpha, \beta).$$

Consider now a given τ' such that $\tau' > S\tau(\omega)$. The expression (5.11) shows that $\bar{e}_{22}(\omega, \tau') > \bar{e}_{22}(\omega, S\tau(\omega)) = \max(\alpha, \beta)$. Therefore we have $\bar{\boldsymbol{e}}(\omega, \tau') \notin C\mathcal{K}^I$ and consequently $\tau' > C\tau(\omega)$. By letting τ' tend towards $S\tau(\omega)$ from above, we obtain that $S\tau(\omega) \geq C\tau(\omega)$. Comparing with (5.13) we can conclude that $S\tau(\omega) = C\tau(\omega)$. For $\omega_1 \leq \omega \leq \pi/4$, the bounds $S\tau$ and $C\tau$ are thus optimal and give the exact value of $Q\tau(\omega)$.

For $\omega < \omega_1$, the numerical results displayed in Figure 7 show that $S_1\tau$ and $S_2\tau$ significantly improve on $S\tau$. In particular, there is an interval $[\omega^*, \omega_1]$ on which the bounds $S_2\tau$ and $C\tau$ are found to coincide (up to the accuracy of the numerical calculations). Let us prove in particular that

$$C\tau(\omega^*) = S_2\tau(\omega^*) = \tau^* \tag{5.14}$$

where

$$\tan 2\omega^* = (\alpha - \beta)/(\delta + 2\epsilon)$$

and

$$\tau^* = \frac{1}{3}\sqrt{(\alpha - \beta)^2 + (\delta + 2\epsilon)^2}.$$

That value τ^* actually corresponds to the maximum of $S_2\tau$ and $C\tau$ (see Figure 7). To prove (5.14) we first note that

$$\bar{\boldsymbol{e}}(\omega^*, \tau^*) = \begin{pmatrix} \frac{\alpha+2\beta}{3} & \frac{\delta+2\epsilon}{3} & 0 \\ \frac{\delta+2\epsilon}{3} & \alpha & 0 \\ 0 & 0 & \frac{2\alpha+\beta}{3} \end{pmatrix}.$$

Observing that $\bar{e}_{22}(\omega^*, \tau^*) = \alpha$ and that $\alpha > \beta$ (in the case of Ni-49.75Ti), we can show that $\tau^* \geq C\tau(\omega^*)$ by a similar reasoning as used previously. We now prove that $\bar{\boldsymbol{e}}(\omega^*, \tau^*)$ is realized by a rank-2 laminate. To that purpose, observe that $\bar{\boldsymbol{e}}(\omega^*, \tau^*)$ can be written as

$$\bar{\boldsymbol{e}}(\omega^*, \tau^*) = \frac{1}{2}(\boldsymbol{e}' + \boldsymbol{e}'') \text{ with } \boldsymbol{e}' = \frac{1}{3}\boldsymbol{e}^I_1 + \frac{2}{3}\boldsymbol{e}^I_9 \text{ and } \boldsymbol{e}'' = \frac{1}{3}\boldsymbol{e}^I_2 + \frac{2}{3}\boldsymbol{e}^I_{12}.$$

Note from Table 1 that $\boldsymbol{e}_1^I$ and $\boldsymbol{e}_9^I$ (resp. $\boldsymbol{e}_2^I$ and $\boldsymbol{e}_{12}^I$) are compatible, so that the strain $\boldsymbol{e}'$ (resp. $\boldsymbol{e}''$) is in $R_1\mathcal{K}^I$. It can be verified that $\det(\boldsymbol{e}' - \boldsymbol{e}'') = 0$, i.e that $\boldsymbol{e}'$ and $\boldsymbol{e}''$ are compatible. Therefore the strain $\bar{\boldsymbol{e}}(\omega^*, \tau^*)$ is in $R_2\mathcal{K}$. As a consequence, we have $\tau^* \leq S_2\tau(\omega^*)$. Combining the obtained relations $C\tau(\omega^*) \leq \tau^* \leq S_2\tau(\omega^*)$ with (5.13), we can conclude that $S_2\tau(\omega^*) = C\tau(\omega^*) = \tau^*$.

The results for the monoclinic-II example (Figure 8) differ in several aspects. A first observation is that, contrary to the case of Ni-49.75Ti, the convex bounds $C\tau$ and $S\tau$ never coincide. As for monoclinic-I martensite, there exists values of ω such that $\max_i \bar{e}_{ii}(\omega, S\tau(\omega)) = \max(\alpha, \beta)$. However, it can no longer be concluded that $\bar{\boldsymbol{e}}(\omega, S\tau(\omega)) \notin C\mathcal{K}^{II}$ for $\tau > S\tau(\omega)$. The reason is that strains $\bar{\boldsymbol{e}}$ in $C\mathcal{K}^{II}$ do not necessarily verify $\bar{e}_{ii} \leq \max(\alpha, \beta)$ (they only satisfy the less stringent restriction $\boldsymbol{e}_{ii} \leq \max(\alpha - \epsilon, \alpha + \epsilon, \beta)$).

A second observation is that the bound $S_2\tau$ improves on $S\tau$ *for all value of* ω. Hence, contrary to the case of monoclinic-I martensite, the convex lower bound $S\tau$ is never optimal. Lastly, concerning upper bounds, we note that $P\tau(\omega)$ is stricly lower than $C\tau(\omega)$ for some values of ω - that situation was not observed in the monoclinic-I example. The numerical calculations show that $C\tau$, $P\tau$ and $S_2\tau$ all reach a maximum at the same value $\omega = \pi/4$. It can be proved that

$$C\tau(\frac{\pi}{4}) = R_2\tau(\frac{\pi}{4}) = \frac{2|\beta - \alpha|}{3}.$$

The proof is similar to the reasoning detailed previously for justifying (5.14). The most delicate point consists in proving that $\bar{\boldsymbol{e}}(\pi/4, 2|\beta - \alpha|/3)$ is in $R_2\mathcal{K}^{II}$. To that purpose, note that

$$\bar{\boldsymbol{e}}(\frac{\pi}{4}, \frac{2|\beta - \alpha|}{3}) = \mathrm{diag}(\beta, \frac{4\alpha - \beta}{3}, \frac{2\alpha + \beta}{3}).$$

That tensor can be written in the form

$$\bar{\boldsymbol{e}}(\frac{\pi}{4}, \frac{2|\beta - \alpha|}{3}) = (\frac{1}{2} - x)\boldsymbol{e}_9^{II} + x\boldsymbol{e}_{10}^{II} + \frac{1}{2}\boldsymbol{e}_{12}^{II},$$

with $x = (\alpha - \beta)/6\epsilon$. The lattice parameters in β_1'Cu-14Al-4Ni satisfy $0 \leq \alpha - \beta \leq 3\epsilon$, so that $x \in [0, 1/2]$. Noting from Table 3 that the strains $\boldsymbol{e}_9^{II}$, $\boldsymbol{e}_{10}^{II}$, $\boldsymbol{e}_{12}^{II}$ are pairwise compatible, we can conclude that $\bar{\boldsymbol{e}}(\pi/4, 2|\beta - \alpha|/3)$ is in $R_2\mathcal{K}$.

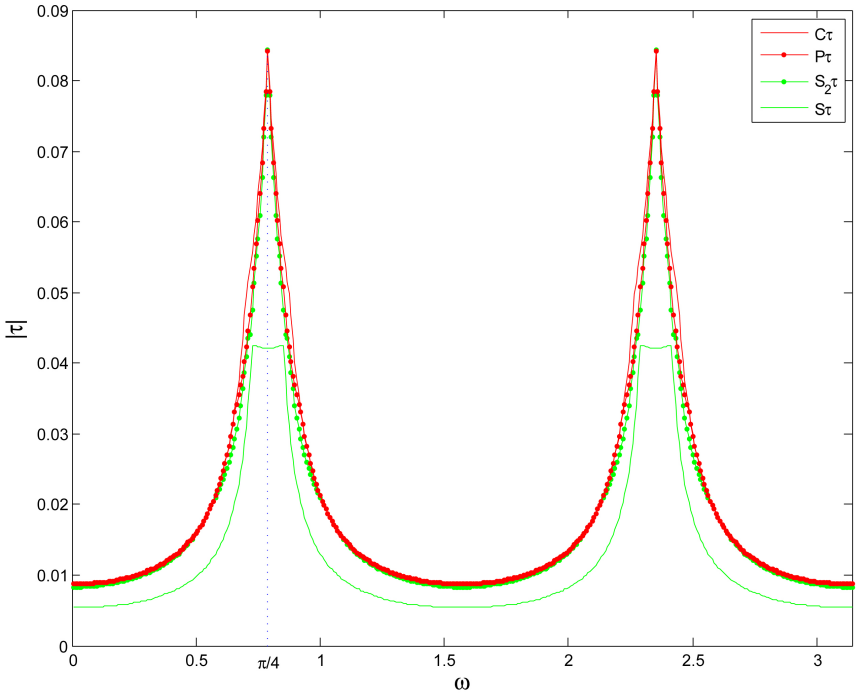

Figure 8: Bounds on (ω, τ) such that $\bar{\boldsymbol{e}}(\omega, \tau) \in Q\mathcal{K}^{II}$.

In the case of β_1'Cu-14Al-4Ni, the functions $P\tau$ and $C\tau$ are very close and therefore give a good approximation of the function $Q\tau$ characterizing the quasiconvex hull. The results for Ni-49.75Ti do not give the same level of closeness between $P\tau$ and $C\tau$, but a significant improvement is still observed compared to the convex lower bound $S\tau$.

In Part 1 of this paper (Peigney, 2013), bounds on the energy-minimizing strains for the cubic to tetragonal transformation have been derived in the geometrically non-linear setting. Those bounds have been illustrated by considering effective strains which are the analogue of (5.10) in the geometrically non-linear theory, i.e. a simple shear (of amplitude τ and orientation ω) applied in the self-accommodated state. The results obtained are qualitatively similar to those displayed in Figure 8: the transformation considered is recoverable up to a maximum shear amplitude $\tau(\omega)$ that depends on ω, the function $\omega \mapsto \tau(\omega)$ exhibiting localized peaks at specific values of ω. Such similarities should not obscure the fact that the arguments at play are of a

different nature. In the geometrically linear example considered in Figure 8, the results that are obtained partly come from the fact that, because we are considering 12 transformation strains, the material is given a large number of degrees of freedom to accommodate a given strain $\bar{\boldsymbol{e}}$. In contrast, if the cubic to tetragonal transformation is studied in the geometrically linear setting, it can easily be verified that the strain $\bar{\boldsymbol{e}}(\omega, \tau)$ is recoverable only for $\tau = 0$. In the geometrically non-linear theory, local rotations act as an additional degree of freedom for the material to accommodate strains. This is the main reason why, even for the cubic to tetragonal transformation, non-zero shear $\tau(\omega)$ is predicted to be recoverable in that theory.

6. Concluding remarks

In difference with the geometrically non-linear theory, the minimizers of the microscopic energy in the geometrically linear theory form a discrete set. This contributes to major simplifications in the analysis. For instance, the upper bound (3.12) for the three-well problem is obtained with relatively simple calculations, whereas considerable effort is needed for the analog bound in the geometrically non-linear theory (Peigney, 2013).

Four- and twelve-well problems have been studied extensively in this paper. There is a connection between the two: for cubic to monoclinic transformations, sufficient conditions on the effective strain $\bar{\boldsymbol{e}}$ can be found for the microstructures to be restricted to only four variants (see Appendix B). In particular, the four-well example $\{\boldsymbol{e}_1, \boldsymbol{e}_2, \boldsymbol{e}_5, \boldsymbol{e}_6\}$ considered in Section 4 can be interpreted as the trace of $Q\mathcal{K}$ on a particular hyperplane of $\{\bar{\boldsymbol{e}} | \operatorname{tr} \bar{\boldsymbol{e}} = 2\alpha + \beta\}$. As notably illustrated on the four-well examples of Section 4.2, the convex upper bound may significantly overestimate the set $Q\mathcal{K}$. It is interesting to observe, however, that it gives a relatively good approximation of $Q\mathcal{K}$ in cubic to monoclinic transformations (especially for monoclinic-I martensite), performing better than the convex lower bound $\mathcal{S}$ in that regard.

The bounds presented could be improved in several ways. For instance, the lower bound $S_2\mathcal{K}$ considered in Section 5 is not stable by lamination. Therefore, the set formed by simple laminates of compatible strains in $S_2\mathcal{K}$ is expected to give a tighter lower bound. Note that the characterization (5.9) of $S_2\mathcal{K}$ is simple enough for such a calculation to remain tractable. It would also be interesting to compare the results presented with the lower bound recently proposed by Chenchiah and Schlömerkemper (2013) for monoclinic-

I martensite. Another interesting line of investigation consists in extending the study to polycrystals.

Appendix A. Proof that $[\boldsymbol{e}_6^{II}, \boldsymbol{e}_8^{II}]$ is a connected component of $Q\mathcal{K}_4^{II}$

In the case $\mathcal{K} = \mathcal{K}_4^{II}$, the mapping f introduced in (4.7) specializes as

$$\begin{array}{rccl} f: & \mathcal{T}_3' & \to & \mathbb{R}_s^{3\times 3} \\ & (\theta_1, \theta_3, \theta_6) & \mapsto & \theta_1 \boldsymbol{e}_1^{II} + \theta_3 \boldsymbol{e}_3^{II} + \theta_6 \boldsymbol{e}_6^{II} + (1 - \sum_{r\in\{1,3,6\}} \theta_r) \boldsymbol{e}_8^{II}. \end{array}$$

Let

$$\begin{array}{rccl} l: & \mathcal{T}_3' & \to & \mathbb{R} \\ & (\theta_1, \theta_3, \theta_6) & \mapsto & \theta_1 + \theta_3. \end{array}$$

Let $\mathcal{C} \subset Q\mathcal{K}_4^{II}$ be a connected subset of $Q\mathcal{K}_4^{II}$ that contains $[\boldsymbol{e}_6^{II}, \boldsymbol{e}_8^{II}]$. Since $f^{-1}l$ is continous, $f^{-1}l(\mathcal{C})$ is a connected set of $\mathbb{R}$, i.e. an interval. Moreover, for any $\boldsymbol{\theta} \in f^{-1}(Q\mathcal{K}_4^{II})$ (resp. $\boldsymbol{\theta} \in f^{-1}([\boldsymbol{e}_6^{II}, \boldsymbol{e}_8^{II}])$), we have $l(\boldsymbol{\theta}) \geq 0$ (resp. $l(\boldsymbol{\theta}) = 0$). It follows that $f^{-1}l(\mathcal{C})$ is an interval of the form $[0, \eta]$ with $\eta \geq 0$. Assume that $\eta > 0$. Then for any $\eta \geq \eta' > 0$, there exists $\boldsymbol{\theta} = \{\theta_1, \theta_3, \theta_6, \theta_8\} \in \mathcal{T}_4$ such that $\sum_{r,s=1,3,6,8} \theta_r\theta_s(\boldsymbol{e}_r^{II} - \boldsymbol{e}_s^{II})^* \leq 0$ and $\theta_1 + \theta_3 = \eta'$. Any such $\boldsymbol{\theta}$ can be written in the form

$$\boldsymbol{\theta} = (x, \eta' - x, y, 1 - \eta' - y),$$

with $0 \leq x \leq \eta'$ and $0 \leq y \leq 1 - \eta'$. Let η' tend towards zero. At the first order in (x, η'), we have

$$\begin{aligned} \frac{1}{2} \sum_{r,s=1,3,6,8} \theta_r\theta_s(\boldsymbol{e}_r^{II} - \boldsymbol{e}_s^{II})^* = \; & xy(\boldsymbol{e}_1^{II} - \boldsymbol{e}_6^{II})^* + x(1-y)(\boldsymbol{e}_1^{II} - \boldsymbol{e}_8^{II})^* \\ & + (\eta' - x)y(\boldsymbol{e}_3^{II} - \boldsymbol{e}_6^{II})^* + (\eta' - x)(1-y)(\boldsymbol{e}_3^{II} - \boldsymbol{e}_8^{II})^* \\ & + y(1 - y - \eta')(\boldsymbol{e}_6^{II} - \boldsymbol{e}_8^{II})^*. \end{aligned}$$

For monoclinic-II martensite, it can easily be verified that $\boldsymbol{u}.(\boldsymbol{e}_6^{II} - \boldsymbol{e}_8^{II})^*.\boldsymbol{u} = 0$ for any $\boldsymbol{u} \in \mathrm{vect}(\boldsymbol{u}_1, \boldsymbol{u}_3)$, and that $\boldsymbol{u}_3.\boldsymbol{e}.\boldsymbol{u}_3 = 2\epsilon(\alpha - \beta - \epsilon) - \delta^2$ for $\boldsymbol{e} \in \{\boldsymbol{e}_1^{II} - \boldsymbol{e}_6^{II}, \boldsymbol{e}_1^{II} - \boldsymbol{e}_8^{II}, \boldsymbol{e}_3^{II} - \boldsymbol{e}_6^{II}, \boldsymbol{e}_3^{II} - \boldsymbol{e}_8^{II}\}$. Therefore we get

$$\frac{1}{2} \sum_{r,s=1,3,6,8} \theta_r\theta_s \boldsymbol{u}_3.(\boldsymbol{e}_r^{II} - \boldsymbol{e}_s^{II})^*.\boldsymbol{u}_3 = \eta'(2\epsilon(\alpha - \beta - \epsilon) - \delta^2).$$

The lattice parameters in β_1'Cu-14Al-4Ni are such that $2\epsilon(\alpha-\beta-\epsilon)-\delta^2>0$. In that case, the relation $\sum_{r,s}\theta_r\theta_s\boldsymbol{u}_3.(\boldsymbol{e}_r^{II}-\boldsymbol{e}_s^{II})^*.\boldsymbol{u}_3\leq 0$ implies that $\eta'=0$, in contradiction with the starting assumption $\eta'>0$. If follows that η is necessarily equal to 0, i.e. that $f^{-1}l(\mathcal{C})=\{0\}$. Any $\boldsymbol{e}$ in $\mathcal{C}$ is such that $\theta_1+\theta_3=0$, i.e. is in $[\boldsymbol{e}_6^{II},\boldsymbol{e}_8^{II}]$. The set $\mathcal{C}$ is thus equal to $[\boldsymbol{e}_6^{II},\boldsymbol{e}_8^{II}]$. This completes the proof that $[\boldsymbol{e}_6^{II},\boldsymbol{e}_8^{II}]$ is a connected component of $Q\mathcal{K}_4^{II}$.

Appendix B. Reduction to four-wells in cubic to monoclinic transformations

Let $\mathcal{K}=\{\boldsymbol{e}_1,\cdots,\boldsymbol{e}_{12}\}$ be the set of transformation strains in a cubic to monoclinic transformation. We examine sufficient conditions on $\bar{\boldsymbol{e}}$ for the microstructures to be restricted on a given set of four variants, say $\{\boldsymbol{e}_1,\boldsymbol{e}_2,\boldsymbol{e}_3,\boldsymbol{e}_4\}$. Assume there exists a tensor $\boldsymbol{N}$ such that

$$\begin{array}{ll}\boldsymbol{e}_r:\boldsymbol{N}=\boldsymbol{e}_1:\boldsymbol{N} & \text{for } r=2,3,4;\\ \boldsymbol{e}_r:\boldsymbol{N}<\boldsymbol{e}_1:\boldsymbol{N} & \text{for } 5\leq r\leq 12.\end{array}\tag{B.1}$$

Consider a given strain $\bar{\boldsymbol{e}}$ in $Q\mathcal{K}$. There exists $\boldsymbol{\theta}\in\mathcal{T}_{12}$ such that $\bar{\boldsymbol{e}}=\sum_{r=1}^{12}\theta_r\boldsymbol{e}_r$. We have

$$\begin{aligned}\bar{\boldsymbol{e}}:\boldsymbol{N} &\leq (\sum_{r=1}^{4}\theta_r)\boldsymbol{e}_1:\boldsymbol{N}+(\sum_{r=5}^{12}\theta_r)\boldsymbol{e}_r:\boldsymbol{N}\\ &\leq (\sum_{r=1}^{4}\theta_r)(\boldsymbol{e}_1:\boldsymbol{N}-\sup_{k>4}\{\boldsymbol{e}_k:\boldsymbol{N}\})+\sup_{k>4}\{\boldsymbol{e}_k:\boldsymbol{N}\}\end{aligned},$$

so that

$$\frac{\bar{\boldsymbol{e}}:\boldsymbol{N}-\sup_{k>4}\boldsymbol{e}_k:\boldsymbol{N}}{\boldsymbol{e}_1:\boldsymbol{N}-\sup_{k>4}\boldsymbol{e}_k:\boldsymbol{N}}\leq\sum_{r=1}^{4}\theta_r.\tag{B.2}$$

Recall that $\boldsymbol{\theta}$ satisfies $\sum_{r=1}^{12}\theta_r=1$ and $\theta_k\geq 0$ for all k. Consequently, if $\bar{\boldsymbol{e}}$ satisfies

$$\bar{\boldsymbol{e}}:\boldsymbol{N}=\boldsymbol{e}_1:\boldsymbol{N},\tag{B.3}$$

then the inequality (B.2) implies that $\sum_{r=1}^{4}\theta_r=1$ and $\theta_k=0$ for $k>4$. Any microstructure realizing $\bar{\boldsymbol{e}}$ is thus necessarily restricted to the four variants $\boldsymbol{e}_1,\boldsymbol{e}_2,\boldsymbol{e}_3,\boldsymbol{e}_4$. To determine if there exists a tensor $\boldsymbol{N}$ satisfying (B.1), consider the affine space W spanned by $\{\boldsymbol{e}_1,\boldsymbol{e}_2,\boldsymbol{e}_3,\boldsymbol{e}_4\}$. Any tensor $\boldsymbol{N}$ satisfying (B.1) is necessarily in the orthogonal $W^{\perp}$ of W in the vectorial

Variants	$(N_{11}, N_{22}, N_{12}, N_{13}, N_{23})$	Variants	$(N_{11}, N_{22}, N_{12}, N_{13}, N_{23})$
(1,2,3,4)	$(0.698, 0.716, 0, 0, 0)$	(1,2,3,7)	$(0.418, 0.216, 0.204, -0.277, 0.277)$
(1,2,3,10)	$(0.216, 0.418, 0.204, -0.277, 0.277)$	(1,2,4,6)	$(0.427, 0.215, 0.203, 0.275, -0.275)$
(1,2,4,11)	$(0.217, 0.41, 0.205, 0.278, -0.278)$	(1,2,5,6)	$(0.267, 0, 0.278, 0.278, -0.278)$
(1,2,5,8)	$(0.696, -0.158, 0.35, 0, 0)$	(1,2,5,12)	$(-0.0417, -0.0417, 0.347, 0.254, -0.254)$
(1,2,6,11)	$(0.13, 0.13, 0.254, 0.298, -0.298)$	(1,2,7,8)	$(0.275, 0, 0.278, -0.278, 0.278)$
(1,2,7,10)	$(0.135, 0.135, 0.252, -0.298, 0.298)$	(1,2,8,9)	$(-0.0407, -0.0407, 0.345, -0.255, 0.255)$
(1,2,9,10)	$(0, 0.254, 0.279, -0.279, 0.279)$	(1,2,9,12)	$(-0.155, 0.707, 0.345, 0, 0)$
(1,2,11,12)	$(0, 0.274, 0.278, 0.278, -0.278)$	(1,3,4,5)	$(0.402, 0.218, -0.205, 0.279, 0.279)$
(1,3,4,9)	$(0.218, 0.403, -0.205, 0.279, 0.279)$	(1,3,5,7)	$(0.822, 0, 0, 0, 0.285)$
(1,3,5,9)	$(0.241, 0.21, -0.197, 0.268, 0.337)$	(1,3,7,10)	$(0.242, 0.205, 0.193, -0.262, 0.345)$
(1,3,9,10)	$(0.138, 0.778, 0, 0, 0.306)$	(1,4,5,6)	$(0.764, 0.142, 0, 0.315, 0)$
(1,4,5,9)	$(0.206, 0.242, -0.194, 0.344, 0.263)$	(1,4,6,11)	$(0.204, 0.242, 0.193, 0.345, -0.262)$
(1,4,9,11)	$(0, 0.825, 0, 0.282, 0)$	(1,5,6,11)	$(0, 0.0444, 0.252, 0.35, -0.252)$
(1,5,7,8)	$(0.223, -0.232, 0.297, -0.219, 0.297)$	(1,5,7,9)	$(0.0347, -0.214, 0.274, -0.201, 0.351)$
(1,5,8,9)	$(-0.0338, -0.246, 0.347, -0.2, 0.272)$	(1,5,9,11)	$(-0.21, 0.039, 0.269, 0.356, -0.198)$
(1,5,9,12)	$(-0.246, -0.0331, 0.346, 0.273, -0.201)$	(1,5,11,12)	$(-0.122, 0, 0.3, 0.3, -0.259)$
(1,7,8,9)	$(0, -0.138, 0.301, -0.254, 0.301)$	(1,7,9,10)	$(0.0482, 0, 0.248, -0.248, 0.355)$
(1,9,11,12)	$(-0.233, 0.202, 0.298, 0.298, -0.22)$		

Table B.7: Reduction to four-wells in Ni-49.75Ti (only groups including variant 1 are listed).

space $V = \{\bar{\boldsymbol{e}} | tr\bar{\boldsymbol{e}} = 2\alpha + \beta\}$. The spaces V and W are respectively of dimension 5 and 3, so that $W^{\perp}$ is of dimension 2. Let $(\boldsymbol{f}_1, \boldsymbol{f}_2)$ denote an orthonormal basis of $W^{\perp}$ and define $\boldsymbol{N}(\omega) = \cos\omega\, \boldsymbol{f}_1 + \sin\omega\, \boldsymbol{f}_2$ for all ω. The system (B.1) admits a solution provided that

$$\sup_{0\leq\omega\leq 2\pi} \{\boldsymbol{e}_1 : \boldsymbol{N}(\omega) - \sup_{k>4} \boldsymbol{e}_k : \boldsymbol{N}(\omega)\} > 0. \tag{B.4}$$

Tables B.7-B.8 list the groups of four variants in Ni-49.75Ti and β_1'Cu-14Al-4Ni that fulfill that condition (B.4), along with the components of a corresponding tensor $\boldsymbol{N}$ satisfying (B.1) (N_{33} is set equal to 0). Those tables are limited to groups including variant 1. Values of the lattice parameters are the same as in Section 5.

References

Ball, J., James, R., 1992. Proposed experimental tests of a theory of fine microstructure and the two-well problem. Phil. Trans. Roy. Soc. London A. 338, 338–450.

Barber, C., Dobkin, D., Huhdanpaa, H., 1996. The quickhull algorithm for convex hulls. ACM Transactions on Mathematical Software 22, 469–483.

Variants	$(N_{11}, N_{22}, N_{12}, N_{13}, N_{23})$	Variants	$(N_{11}, N_{22}, N_{12}, N_{13}, N_{23})$
(1,2,5,6)	$(0, 0, 0.354, 0.354, 0.00469)$	(1,2,5,10)	$(0.0865, 0.0865, 0.154, 0.334, 0.334)$
(1,2,5,12)	$(0.0877, 0.0877, 0.152, 0.334, -0.334)$	(1,2,6,9)	$(-0.0616, -0.0616, 0.472, 0.113, 0.113)$
(1,2,6,11)	$(-0.0598, -0.0598, 0.468, 0.12, -0.12)$	(1,2,7,8)	$(0, 0, 0.354, -0.354, 0.00116)$
(1,2,7,10)	$(0.0868, 0.0868, 0.154, -0.334, 0.334)$	(1,2,7,12)	$(0.0834, 0.0834, 0.159, -0.332, -0.332)$
(1,2,8,9)	$(-0.0614, -0.0614, 0.471, -0.114, 0.114)$	(1,2,8,11)	$(-0.062, -0.062, 0.472, -0.112, -0.112)$
(1,2,9,10)	$(0, 0, 0.354, 0.000358, 0.354)$	(1,2,11,12)	$(0, 0, 0.354, 0.007, -0.354)$
(1,3,5,7)	$(1, 0, 0, 0, 0.00627)$	(1,3,5,10)	$(0.124, 0.0653, 0, 0.136, 0.476)$
(1,3,5,12)	$(0.123, 0.0644, 0, 0.134, -0.477)$	(1,3,7,10)	$(0.12, 0.0588, 0, -0.122, 0.48)$
(1,3,7,12)	$(0.123, 0.0644, 0, -0.134, -0.477)$	(1,5,6,9)	$(0, -0.0866, 0.335, 0.155, 0.335)$
(1,5,6,11)	$(0, -0.0823, 0.333, 0.162, -0.333)$	(1,5,7,9)	$(0.0598, -0.0635, 0.132, 0, 0.48)$
(1,5,7,11)	$(0.0601, -0.0629, 0.13, 0, -0.481)$	(1,5,9,10)	$(0.0608, 0, 0.117, 0.117, 0.471)$
(1,5,11,12)	$(0.0617, 0, 0.113, 0.113, -0.473)$	(1,6,8,9)	$(-0.0595, -0.123, 0.478, 0, 0.131)$
(1,6,8,11)	$(-0.0595, -0.123, 0.478, 0, -0.131)$	(1,7,8,9)	$(0, -0.0833, 0.334, -0.161, 0.334)$
(1,7,8,11)	$(0, -0.0868, 0.335, -0.155, -0.335)$	(1,7,9,10)	$(0.0616, 0, 0.114, -0.114, 0.472)$
(1,7,11,12)	$(0.062, 0, 0.112, -0.112, -0.473)$		

Table B.8: Reduction to four-wells in β_1'Cu-14Al-4Ni (only groups including variant 1 are listed).

Bhattacharya, K., 1993. Comparison of the geometrically nonlinear and linear theories of martensitic transformations. Contin.Mech.Thermodyn. 5, 205–242.

Bhattacharya, K., Kohn, R., 1997. Energy minimization and the recoverable strains in polycrystalline shape memory alloys. Arch. Rational Mech. Anal. 139, 99–180.

Chakravorty, S., Wayman, C., 1977. Electron microscopy of internally faulted CuZnAl martensite. Acta Metall. 25, 989–1000.

Chenchiah, I., Schlömerkemper, A., 2013. Non-laminate microstructures in monoclinic-I martensite. Arch. Rational Mech. Anal. 207, 39–74.

Dacorogna, B., 2008. Direct methods in the calculus of variations, second edition. Springer.

Govindjee, S., Hackl, K., Heinen, R., 2007. An upper bound to the free energy of mixing by twin-compatible lamination for n-variant martensitic phase transformations. Continuum Mech. Thermodyn. 18, 443–453.

Govindjee, S., Mielke, A., Hall, G., 2003. The free energy of mixing for $n-$variant martensitic phase transformations using quasi-convex analysis. J. Mech. Phys. Solids 51, I–XXVI.

Kinderlehrer, D., Pedregal, P., 1991. Characterizations of young measures generated by gradients. Arch. Rational Mech. Anal. 115, 329–365.

Knowles, K., Smith, D., 1981. Crystallography of the martensitic transformation in equiatomic nickel-titanium. Acta Mater. 29, 101–110.

Kohn, R., 1991. Relaxation of a double-well energy. Continuum Mech. Thermodyn. 3, 193–236.

Müller, S., 1999. Variational models for microstructure and phase transitions. In: Calculus of variations and geometric evolution problems. Springer.

Peigney, M., 2008. Recoverable strains in composite shape-memory alloys. J. Mech. Phys. Solids 56, 360–375.

Peigney, M., 2009. A non-convex lower bound on the effective free energy of polycrystalline shape memory alloys. J. Mech. Phys. Solids 57, 970–986.

Peigney, M., 2013. On the energy-minimizing strains in martensitic microstructures - Part 1: geometrically non-linear theory. J. Mech. Phys. Solids 61, 1489–1510.

Saburi, T., Nenno, S., Kato, S., Takata, K., 1976. Configurations of martensite variants in Cu-Zn-Ga. J. Less Common Metals 50, 223–236.

Seo, J., Schryvers, D., 1998. Tem investigation of the microstructure and defects of CuZr martensite. Acta Mater. 46, 1177–1183.

Shu, Y., Bhattacharya, K., 1998. The influence of texture on the shape-memory effects in polycrystals. Acta Mater. 15, 5457–5473.

Smyshlyaev, V., Willis, J., 1998. On the relaxation of a three-well energy. Proc. R. Soc. Lond. A 455, 779–814.

Tadaki, T., Tokoro, M., Shimizu, K., 1975. Thermoelastic nature and crystal structure of the Cu-Zn martensite related to the shape memory alloy. Trans. Jap. Inst. Metals 56, 285–296.